Regular Article

Control of atmospheric carbon dioxide level through integrated carbon taxation-reforestation policy: a modeling study

Maitri Verma[1,a] , **Cherie Gautam**[1], **Kalyan Das**[2]

[1] Department of Mathematics, School of Physical and Decision Sciences, Babasaheb Bhimrao Ambedkar University, Lucknow 226025, India
[2] Department of Basic and Applied Sciences, National Institute of Food Technology Entrepreneurship and Management, Kundli, Haryana 131028, India

Abstract Global warming is a serious issue that affects the environment and mankind. The anthropogenic emissions of carbon dioxide, mainly due to fossil fuel burning and deforestation, are among the root cause of global warming. The goal of this work is to present a mathematical model to analyze the long-term impact of an integrated CO_2 taxation-reforestation policy on the mitigation of atmospheric CO_2 levels. It is assumed that carbon tax is applied to anthropogenic CO_2 emissions and a part of the money generated by carbon taxation is invested to accelerate the reforestation programs. The stability theory of differential equations is applied to examine the qualitative behaviour of the system. Lyapunov stability theory is used to derive sufficient conditions under which the atmospheric carbon dioxide level gets stabilized. It is found that an increment in the deforestation rate coefficient above a threshold level leads to stability loss of interior equilibrium and generation of periodic orbits via Hopf-bifurcation. It is found that the amplitude of the oscillation cycles can be dampened on increasing the maximum efficiency of reforestation programs to increase the forest biomass and above a threshold value of the maximum efficiency of reforestation programs, the periodic oscillations die out. It is found that the seasonality in the application of reforestation efforts may lead to the generation of higher periodic solutions above a threshold level of deforestation rate, making it hard to predict and control the atmospheric CO_2 level. The conditions for global attractivity of positive periodic solution of the seasonally forced model are discussed. Numerical simulation has been presented to illustrate the theoretical findings.

1 Introduction

The unprecedented increase in the radiative forcing of Earth's atmosphere over the last few decades has given rise to the threat of global warming. The anthropogenic carbon dioxide emission is the prime contributor to the increase in the radiative forcing of the Earth's atmosphere. Every year human activities, mainly deforestation and fossil fuel burning, are putting more carbon dioxide (CO_2) into the atmosphere than natural processes can remove. The excessive anthropogenic CO_2 emissions have pushed the atmospheric CO_2 above the level of 400 ppm, the highest at any time in the past 800,000 years [1]. Deforestation is one of the prime causes behind the upsurge in CO_2 concentrations. Agricultural expansion, logging for fuel, fodder, wood, and paper-based industries, and infrastructure expansion to support the growing population and economy are mainly attributed to deforestation. Between 1990 and 2020, 420 million ha (hectare) of forest was lost because of deforestation [2]. With the growth in the world's population and economy, the deforestation rate is expected to further increase due to agriculture and infrastructure expansion. In this scenario, restoring the forest cover is imperative to tackle the climate changes caused by enhanced levels of atmospheric carbon dioxide. Many countries are implementing forest conservation policies to enlarge their forest cover. The adoption of forest conservation policies can have a profound impact on forest biomass conservation and even cause the reversal of deforestation trends. For instance, Costa Rica has achieved success in reversing deforestation by increasing the forest cover from 24.4% in 1985 to more than 50% by 2011 by implementing the forest conservation programs [3]. Reforestation programs are prominent options to restore the forest cover; but their implementation on a desired scale involves many economical and geographical constraints [4]. One of the constraints is the economic cost of planting and managing the forests.

Apart from deforestation, fossil fuel burning for energy generation and industrial processes is another prominent source of CO_2 emissions. Many countries, such as Canada, South Africa, India, Taiwan, Columbia, Costa Rica and most EU countries, have implemented environmental regulations to reduce carbon emissions by imposing taxes [5]. The taxation policy is corroborated by the government to directly price the emissions of carbon dioxide of enterprises, following the taxation principle of "who consumes, who pays" [6]. The implementation of carbon taxation is an effective option to reduce the carbon dioxide emissions from the point source. Several empirical, semi-empirical and numerical models are used to study the nexus between carbon taxation and carbon

---

[a] e-mail: maitri.verma9@gmail.com (corresponding author)

Fig. 1 The flowchart of the methodology
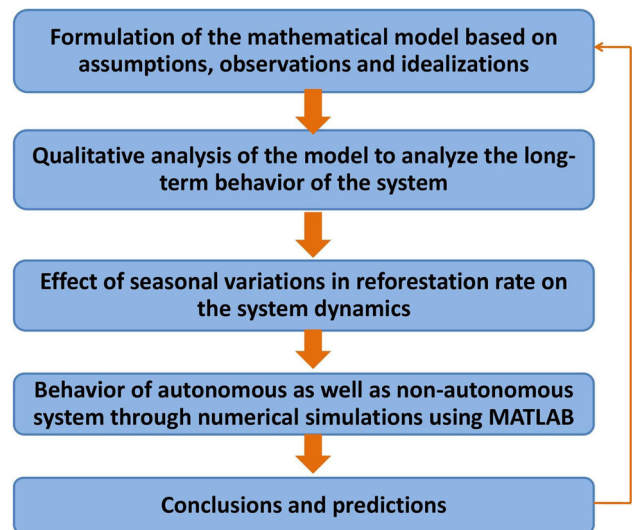
dioxide emissions from anthropogenic sources [7–15]. These studies pointed out that carbon taxation is effective strategy to mitigate the carbon dioxide levels. In particular, Andersson [12] has used an empirical model to quantify the effect of the implementation of a carbon tax and a value-added tax on transport fuel in Sweden and showed that the implementation of the carbon tax and a value-added tax causes a reduction of nearly 11 percent in carbon dioxide emissions from transport. Ghazounani et al. [14] have also empirically analyzed the effect of a carbon tax on the mitigation of carbon dioxide emissions in the European context and showed a significant and positive effect of adoption of a carbon tax on the reduction of CO_2 emissions. However, these studies provide a quantitative analysis of the effect of carbon taxation on the control of carbon dioxide emissions and rely entirely on the data. Apart from these numerical and empirical models, theoretical models that employ qualitative methods can be used to gain an in-depth understanding of the effect of carbon taxation on the control of anthropogenic carbon dioxide emissions. In recent years, various differential equation models have been proposed and analyzed qualitatively to study the impact of human activities and forest biomass over the dynamics of carbon dioxide in the atmosphere [16–30]. In particular, Misra et al. [20] have proposed a mathematical model to analyze the effect of reforestation and the delay involved in between the measurement of forest data and implementation of reforestation efforts on the control of carbon dioxide concentration in the atmosphere. Misra and Jha [27] have proposed a nonlinear model to study the effect of population pressure on the dynamics of carbon dioxide. Their study reveals that as the reduction rate coefficient of carrying capacity of forest biomass due to population pressure increases, the equilibrium level of atmospheric carbon dioxide increases. Verma and Gautam [29] have proposed and analyzed a nonlinear mathematical model to study the effect of forest management programs on the control of atmospheric carbon dioxide. This study indicates that the atmospheric carbon dioxide level can be reduced by increasing the implementation rate and maximum efficiencies of forest management options to reduce deforestation rate and increase forest biomass, respectively. Devi and Gupta [31] have proposed a mathematical model to analyze the effect of environmental tax and time lag in implementation of taxation policy on the concentration of greenhouse gases. This study shows that the concentration of greenhouse gases can be reduced to innocuous level via increasing the implementation rate of environment tax. The literature review shows that there is lack of mathematical studies that analyze the long-term effect of integrated carbon taxation-reforestation policies on the atmospheric CO_2 levels. However, such a study is very important as the integration of carbon taxation and reforestation policies may aid in overcoming the economic constraints that exist in large scale tree plantation. The goal of the present work is to propose and analyze a nonlinear mathematical model to explore the effect of a mitigation policy that integrates the reforestation programs with carbon taxation on the atmospheric CO_2. We assumed that the carbon tax is applied to the anthropogenic emission of carbon dioxide that result in the reduction of CO_2 emissions from the point source. Further, a portion of the fund collected through taxation is spent to accelerate reforestation programs. Since the reforestation efforts are subjected to the seasonal variations, the model is further extended to incorporate seasonality in implementation of reforestation programs by taking the implementation rate of reforestation programs as periodic function of time.

The remainder of this paper is ordered as follows. The next section presents the formulation of mathematical model used to examine the effects of the integrated carbon taxation -reforestation policy on the control of carbon dioxide levels. In Sect. 3, the boundedness of model solutions is discussed. Further, the feasible equilibrium points of the model are identified and their stability properties are examined. The existence of Hopf-bifurcation is discussed by taking the deforestation rate coefficient of forest biomass as a bifurcation parameter. Section 4 offers the study of the effect of seasonal variations in reforestation rate over the system dynamics. We have demonstrated the behavior of autonomous as well as nonautonomous system through numerical simulations in Sect. 5. Finally, Sect. 6 concludes the important findings of the work. A flowchart of the methodology is given in Fig. 1.

2 The model

Let in a geographical region, $C(t)$ denotes the atmospheric concentration of CO_2 at any time t. Further, let $N(t)$ and $B(t)$ denote the human population and forest biomass, respectively. Let $T(t)$ and $R(t)$ denote the carbon tax and a measure of reforestation programs, respectively at time t. The reforestation programs are measured in terms of money invested in their implementation. We formulate a mathematical model to study the effect of the integrated carbon taxation-reforestation policy on the dynamics of atmospheric CO_2 based on the following assumptions:

  (i)   The natural emission rate of CO_2 is constant while the anthropogenic emission rate of CO_2 is proportional to the human population [32, 33].
  (ii) The removal rate of CO_2 by forests during photosynthesis process depends on the carbon dioxide concentration and the forest biomass, while the removal rate of carbon dioxide by natural sinks other than forests is proportional to CO_2 concentration [34].
  (iii) The population and forest biomass are assumed to evolve with time according to logistic growth law. The population clears forest for their use which feeds back to the population growth [35]. So, it is considered that the forest biomass's growth rate declines because of increase in population and population's growth rate boosts because of increase in forest biomass.
  (iv) It is assumed that the population declines due to the adverse impacts of climate changes caused by the enhancement in the concentration of CO_2 [19].
  (v)   The implementation of reforestation programs causes increase in forest biomass. Since the forest biomass can not increase indefinitely with the increase in reforestation programs, so the increment in the forest biomass due to reforestation program is taken as a increasing saturating function of reforestation programs.
  (vi) Carbon tax is assumed to be applied to the anthropogenic CO_2 emission at a rate proportional to the anthropogenic CO_2 emission rate. The application of carbon tax leads to the reduction in the anthropogenic CO_2 emission rate. Since, the reduction in anthropogenic CO_2 emission rate brought by carbon taxation can not increase indefinitely with carbon taxation, therefore it is taken as a increasing saturating function of carbon tax.
  (vii) It is assumed that some taxation policies will be scraped with time due to their inefficacy.
  (viii) The reforestation programs are executed with a rate proportional to the difference between the carrying capacity of forest biomass and its current density. A portion of carbon tax is invested on reforestation programs that enhance the implementation rate of reforestation programs. Further, it is considered that some reforestation programs are diminished due to their inefficiency or some economical barriers.

The above assumptions give rise to the following system of differential equations governing the time evolutions of the model variables:

$$
\begin{aligned}
\dot{C} &= Q + \lambda\left(1 - \frac{\eta T}{l + T}\right)N - \alpha C - \lambda_1 BC, \\
\dot{N} &= sN\left(1 - \frac{N}{L}\right) - \theta CN + \xi NB, \\
\dot{B} &= uB\left(1 - \frac{B}{M}\right) - \phi NB + \frac{\beta RB}{p + R}, \\
\dot{T} &= \gamma(\lambda N) - \gamma_0 T, \\
\dot{R} &= (\delta_1 + \delta_2 T)(M - B) - \delta_0 R,
\end{aligned}
\tag{1}
$$

with initial conditions $C(0) > 0$, $N(0) \geq 0$, $B(0) \geq 0$, $T(0) \geq 0$ and $R(0) \geq 0$. The parameters used in system (1) are specified in Table 1.

3 Qualitative analysis of the system (1)

Since the model system (1) is highly non-linear, it is not possible to find the exact solution to the system. Instead, we will determine the long-term behaviour of the system by applying the stability theory of ordinary differential equations. In this regard, we will determine the feasible equilibrium states of the system (1) and examine their stability properties.

3.1 Boundedness

Boundedness of a system demonstrates that it is well behaved, and ensures that the model variables will not grow exponentially as time increases indefinitely. The results regarding the boundedness of the solution of model system (1) are given in following Lemma 1.

Lemma 1 *The region of attraction [36] for the solution of the system (1) initiating in the positive cone of* $\mathbb{R}^5$ *is given by the set*

Table 1 Description and values of the model parameters of system (1) with their unit and source

Parameter	Description	Values with unit	Source
Q	Natural emission rate of carbon dioxide	1 ppm month^{-1}	[19]
λ	Anthropogenic emission rate coefficient of CO_2	0.05 ppm person^{-1} month^{-1}	[19]
η	Maximum efficacy of carbon taxation programs to reduce the anthropogenic CO_2 emission rate	0.3	Assumed
l	Half saturation constant representing the level of carbon taxation at which half of maximum efficacy of carbon taxation programs to reduce the anthropogenic CO_2 emission rate is attained	300 million dollar	Assumed
α	Removal rate coefficient of atmospheric CO_2 by natural sinks	0.003 month^{-1}	[19]
λ_1	Removal rate coefficient of atmospheric CO_2 by forest biomass	0.0001 ton^{-1} month^{-1}	[19]
ξ	Growth rate coefficient of the population due to the forest biomass	0.000001 ton^{-1} month^{-1}	Assumed
s	Intrinsic growth rate of human population	0.01 month^{-1}	[19]
L	Carrying capacity of human population	1000 person	[19]
θ	Declination rate coefficient of population due to increase in atmospheric CO_2	0.00001 ppm^{-1} month^{-1}	[19]
ϕ	Deforestation rate coefficient	0.0003 person^{-1} month^{-1}	[19]
u	Intrinsic growth rate of forest biomass	0.2 month^{-1}	[19]
M	Carrying capacity of forest biomass	2000 ton	[19]
β	Maximum efficiency of reforestation programs to enhance forest biomass	0.2 month^{-1}	Assumed
p	Half saturation constant representing the reforestation programs at which half of maximum efficiency of reforestation programs to enhance forest biomass is attained	400 million dollar	Assumed
γ	Imposition rate coefficient of carbon tax	0.4 million dollar ppm^{-1}	Assumed
γ_0	Declination rate coefficient of carbon tax	0.015 month^{-1}	Assumed
δ_1	Implementation rate coefficient of reforestation programs	1 million dollar ton^{-1} month^{-1}	Assumed
δ_2	Expenditure rate of carbon tax on reforestation programs	0.001 ton^{-1} month^{-1}	Assumed
δ_0	Declination rate coefficient of reforestation programs	4 month^{-1}	Assumed

$$\Gamma = \{(C, N, B, T, R) \in \mathbb{R}_+^5 : 0 < C \le C_m; 0 \le N \le N_m; 0 \le B \le B_m; 0 \le T \le T_m; 0 \le R \le R_m\},$$

where $C_m = \frac{Q+\lambda N_m}{\alpha}$, $N_m = \frac{L}{s}(s + \xi M)$, $B_m = M$, $T_m = \frac{\gamma \lambda N_m}{\gamma_0}$ and $R_m = \frac{(\delta_1 + \delta_2 T_m)M}{\delta_0}$, which is invariant with respect to system (1).

Proof From third equation of system (1), we have

$$\frac{dB}{dt} \le uB\left(1 - \frac{B}{M}\right) + \frac{\beta R B}{p + R}.$$

From the last equation of model system (1), we note that as B increases to M, R becomes zero, suggesting that $\frac{dB}{dt} \le 0$ for $B \ge M$. Thus, $B \to M$ for large $t > 0$.

$$\Rightarrow \limsup_{t \to \infty} B(t) \le M = B_m \ (say),$$

From second equation of system (1), we have

$$\frac{dN}{dt} \le sN - \frac{sN^2}{L} + \xi NM.$$

$$\Rightarrow \limsup_{t \to \infty} N(t) \le \frac{L}{s}(s + \xi M) = N_m \ (say),$$

From first equation of system (1), we have

$$\frac{dC}{dt} \le Q + \lambda N_m - \alpha C.$$

$$\Rightarrow \limsup_{t \to \infty} C(t) \le \frac{Q + \lambda N_m}{\alpha} = C_m \ (say),$$

From fourth equation of system (1), we have

$$\frac{dT}{dt} \le \gamma \lambda N_m - \gamma_0 T.$$

$$\Rightarrow \limsup_{t \to \infty} T(t) \le \frac{\gamma \lambda N_m}{\gamma_0} = T_m \ (say),$$

From fifth equation of system (1), we have

$$\frac{dR}{dt} \le (\delta_1 + \delta_2 T_m)M - \delta_0 R$$

$$\Rightarrow \limsup_{t \to \infty} R(t) \le \frac{(\delta_1 + \delta_2 T_m)M}{\delta_0} = R_m \ (say).$$

This proves the lemma. $\qquad\qquad\qquad\qquad\qquad\qquad\qquad\qquad\qquad\qquad\qquad\qquad\qquad\qquad\qquad\quad\square$

3.2 Equilibria

An equilibrium point of dynamical system (1) represents the state of the system which does not change with time. The equilibrium states of system (1) are obtained by putting the rate of change of all dynamical variables with respect to time $'t'$ equal to zero. It is found that system (1) has four feasible equilibria; three boundary equilibria and one interior equilibrium.

3.2.1 Boundary equilibria

System (1) has three feasible boundary equilibria, which are given below:

1. $S_1\left(\frac{Q}{\alpha}, 0, 0, 0, \frac{\delta_1 M}{\delta_0}\right)$ always exists.
2. $S_2\left(\frac{Q}{\alpha + \lambda_1 M}, 0, M, 0, 0\right)$ always exists.
3. $S_3(C_3, N_3, 0, T_3, R_3)$ exists provided

$$s > \frac{\theta Q}{\alpha}, \tag{2}$$

The existence of the boundary equilibria S_1 and S_2 are obvious. In the equilibrium $S_3(C_3, N_3, 0, T_3, R_3)$, the values of C_3, N_3, T_3 and R_3 are found by solving the given set of differential equations:

$$Q + \lambda\left(1 - \frac{\eta T}{l + T}\right)N - \alpha C = 0, \tag{3}$$

$$s\left(1 - \frac{N}{L}\right) - \theta C = 0, \tag{4}$$

$$\gamma(\lambda N) - \gamma_0 T = 0, \tag{5}$$

$$(\delta_1 + \delta_2 T)M - \delta_0 R = 0. \tag{6}$$

From the equation (5), we have

$$T = \frac{\gamma \lambda N}{\gamma_0}. \tag{7}$$

Using equation (7) in equation (6), we have

$$R = \frac{M}{\delta_0}\left(\delta_1 + \frac{\delta_2 \gamma \lambda N}{\gamma_0}\right). \tag{8}$$

Using Eq. (7) in Eq. (3), we have

$$C = \frac{1}{\alpha}\left[Q + \lambda N\left(\frac{l\gamma_0 + \gamma \lambda N(1-\eta)}{l\gamma_0 + \gamma \lambda N}\right)\right]. \tag{9}$$

Using Eq. (9) in Eq. (4), we have a two degree polynomial in N

$$\hat{a}N^2 + \hat{b}N + \hat{c} = 0 \tag{10}$$

where $\hat{a} = \frac{s\gamma\lambda}{L} + \frac{\gamma\lambda^2\theta(1-\eta)}{\alpha}$, $\hat{b} = \frac{sl\gamma_0}{L} + \frac{\theta\lambda(l\gamma_0+\gamma Q)}{\alpha} - s\gamma\lambda$ and $\hat{c} = -l\gamma_0\left(s - \frac{\theta Q}{\alpha}\right)$. Clearly, $\hat{a} > 0$ and $\hat{c} < 0$ provided $s - \frac{\theta Q}{\alpha} > 0$. Thus, a unique positive root of N, say N_3, of Eq. (10) exists provided condition (2) holds. Putting $N = N_3$ in Eqs. (7), (8) and (9), we get the positive values of $T = T_3$, $R = R_3$ and $C = C_3$, respectively.

3.2.2 Interior equilibrium

The components of interior equilibrium $S^*(C^*, N^*, B^*, T^*, R^*)$ are obtained by solving the following equations:

$$Q + \lambda\left(1 - \frac{\eta T}{l+T}\right)N - \alpha C - \lambda_1 BC = 0, \tag{11}$$

$$s\left(1 - \frac{N}{L}\right) - \theta C + \xi B = 0, \tag{12}$$

$$u\left(1 - \frac{B}{M}\right) - \phi N + \frac{\beta R}{p+R} = 0, \tag{13}$$

$$\gamma(\lambda N) - \gamma_0 T = 0, \tag{14}$$

$$(\delta_1 + \delta_2 T)(M - B) - \delta_0 R = 0, \tag{15}$$

From Eq. (14), we have

$$T = \frac{\gamma \lambda N}{\gamma_0}. \tag{16}$$

Using this value of T in Eqs. (11) and (15), we get

$$C = \frac{1}{\alpha + \lambda_1 B}\left[Q + \lambda N\left(1 - \frac{\eta\gamma\lambda N}{l\gamma_0 + \gamma \lambda N}\right)\right]. \tag{17}$$

and

$$R = \left(\frac{M-B}{\delta_0}\right)\left(\delta_1 + \frac{\delta_2\gamma\lambda N}{\gamma_0}\right). \tag{18}$$

Using Eq. (17) in Eq. (12), we get the following equation in N and B:

$$s\left(1 - \frac{N}{L}\right) - \frac{\theta}{\alpha + \lambda_1 B}\left[Q + \lambda N\left(1 - \frac{\eta\gamma\lambda N}{l\gamma_0 + \gamma \lambda N}\right)\right] + \xi B = 0. \tag{19}$$

Using Eq. (18) in Eq. (13), we get another equation in N and B as:

$$u\left(1 - \frac{B}{M}\right) - \phi N + \frac{\beta\left(\frac{M-B}{\delta_0}\right)\left(\delta_1 + \frac{\delta_2\gamma\lambda N}{\gamma_0}\right)}{p + \left(\frac{M-B}{\delta_0}\right)\left(\delta_1 + \frac{\delta_2\gamma\lambda N}{\gamma_0}\right)} = 0. \tag{20}$$

Now to establish the existence of S^*, we plot the isoclines given by Eqs. (19) and (20).
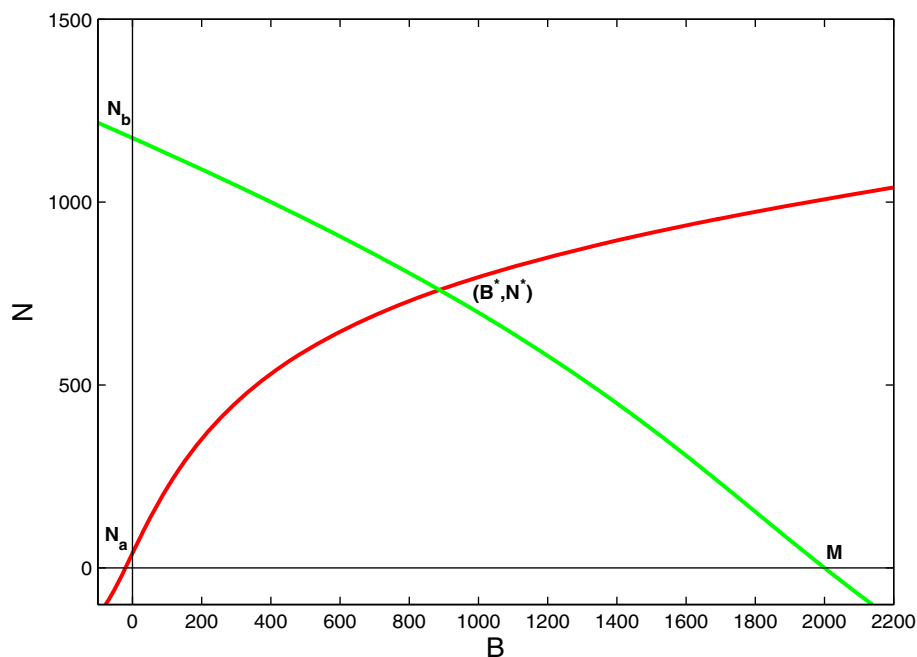
From Eq. (19), we may noted that:

(i) When $N = 0$, we get the following quadratic equation in B

$$\xi\lambda_1 B^2 + (s\lambda_1 + \xi\alpha)B + (s\alpha - \theta Q) = 0,$$

which has negative roots under the condition (2).

Fig. 2 Intersection of the isoclines (19) (shown by red colour) and (20) (shown by green colour) at a unique point (B^*, N^*) in the region $\Omega' = \{(B, N) \in \mathbb{R}_+^2 : 0 \leq B \leq M, N \geq 0\}$ of positive quadrant

(ii) When $B = 0$, we get the following equation in N:

$$\left(\frac{s\gamma\lambda}{L} + \frac{\gamma\lambda^2\theta(1-\eta)}{\alpha}\right)N^2 - \left[\left(s - \frac{\theta Q}{\alpha}\right)\gamma\lambda - l\gamma_0\left(\frac{s}{L} + \frac{\lambda\theta}{\alpha}\right)\right]N - l\gamma_0\left(s - \frac{\theta Q}{\alpha}\right) = 0.$$

This equation has unique positive root, say N_a provided the condition (2) holds.

(iii) $\frac{dN}{dB} > 0$.

Similarly, from Eq. (20), we may noted that:

(i) When $N = 0$, we get $B = M$.

(ii) When $B = 0$, we get the following equation in N:

$$\frac{\delta_2\phi\gamma\lambda M}{\delta_0\gamma_0}N^2 - \left[\frac{u\delta_2\gamma\lambda M}{\delta_0\gamma_0} - \phi\left(p + \frac{\delta_1 M}{\delta_0}\right) + \frac{\beta M\delta_2\gamma\lambda}{\gamma_0\delta_0}\right]N - \left[u\left(p + \frac{\delta_1 M}{\delta_0}\right) + \frac{\beta M\delta_1}{\delta_0}\right] = 0.$$

The above equation has unique positive root, say N_b.

(iii) $\frac{dN}{dB} < 0$.

Now, the isoclines given by (19) and (20) will intersect at a unique point (B^*, N^*) in the region $\Omega' = \{(B, N) \in \mathbb{R}_+^2 : 0 \leq B \leq M, N \geq 0\}$ of positive quadrant as shown in Fig. 2 provided

$$N_b > N_a. \tag{21}$$

Using the values of N^* and B^* in (16), (17) and (18), we get the positive value of $T = T^*$, $C = C^*$ and $R = R^*$, respectively. Thus, a unique interior equilibrium S^* exists under the conditions (2) and (21).

3.3 Local stability analysis

In order to examine the faith of solution trajectories of the system (1) initiating in small neighborhood of the non-negative equilibria S_1, S_2, S_3 and S^*, the local stability analysis is performed. The local stability analysis tells about the faith of solution trajectories that initiated close to but not precisely at the equilibrium point. The local stability behavior of equilibrium points is investigated by determining the sign of the eigenvalues of Jacobian matrix evaluated at the equilibrium points [37] and the following result is obtained:

Theorem 1 *(i) The equilibrium S_1 is unstable.*

(ii) The equilibrium S_2 is unstable whenever S^* exists.

(iii) The equilibrium S_3 is unstable whenever $u - \phi N_3 + \frac{\beta R_3}{p+R_3} > 0$.

(iv) *The equilibrium S^* is locally asymptotically stable if and only if conditions stated below hold:*

$$A_5 > 0, \ A_1 A_2 - A_3 > 0, \ A_3(A_1 A_2 - A_3) - A_1(A_1 A_4 - A_5) > 0,$$
$$A_4\{A_3(A_1 A_2 - A_3) - A_1(A_1 A_4 - A_5)\} - A_5\{A_2(A_1 A_2 - A_3) - (A_1 A_4 - A_5)\} > 0. \tag{22}$$

where $A_i's (i = 1, 2, 3, 4, 5)$ are defined in the proof.

Proof The variational matrix J for system (1) is given as

$$J = \begin{pmatrix} J_{11} & J_{12} & J_{13} & J_{14} & 0 \\ J_{21} & J_{22} & J_{23} & 0 & 0 \\ 0 & J_{32} & J_{33} & 0 & J_{35} \\ 0 & J_{42} & 0 & J_{44} & 0 \\ 0 & 0 & J_{53} & J_{54} & J_{55} \end{pmatrix},$$

where $J_{11} = -(\alpha + \lambda_1 B), \ J_{12} = \lambda\left(1 - \frac{\eta T}{l+T}\right), \ J_{13} = -\lambda_1 C, \ J_{14} = -\frac{\lambda \eta l N}{(l+T)^2}$,

$J_{21} = -\theta N, \ J_{22} = s\left(1 - \frac{2N}{L}\right) - \theta C + \xi B, \ J_{23} = \xi N$,

$J_{32} = -\phi B, \ J_{33} = u\left(1 - \frac{2B}{M}\right) - \phi N + \frac{\beta R}{p+R}, \ J_{35} = \frac{\beta p B}{(p+R)^2}$,

$J_{42} = \gamma \lambda, \ J_{44} = -\gamma_0, \ J_{53} = -(\delta_1 + \delta_2 T), \ J_{54} = \delta_2(M - B), \ J_{55} = -\delta_0$. Let $J_{S_1}, J_{S_2}, J_{S_3}$ and J_{S^*} denote the variational matrix J evaluated at S_1, S_2, S_3 and S^*, respectively. Then we have

(i) The eigenvalues of matrix J_{S_1} are $-\alpha, \ s - \frac{\theta Q}{\alpha}, \ u + \frac{\beta \delta_1 M}{p \delta_0 + \delta_1 M}, \ -\gamma_0, \ -\delta_0$. It is clear that one value is $u + \frac{\beta \delta_1 M}{p \delta_0 + \delta_1 M}$, which is always positive and hence S_1 is always unstable.

(ii) The eigenvalues of J_{S_2} are $-(\alpha + \lambda_1 M), \ s - \frac{\theta Q}{\alpha + \lambda_1 M} + \xi M, \ -\gamma_0$ and the other two values are the roots of the quadratic equation $\hat{\psi}^2 + (u + \delta_0)\hat{\psi} + u\delta_0 + \frac{\beta M \delta_1}{p} = 0$, which are either negative or with negative real part. It is clear that one value of J_{S_2} is $s - \frac{\theta Q}{\alpha + \lambda_1 M} + \xi M$, which is positive whenever S^* exists. Thus, the equilibria S_2 is unstable whenever S^* exists.

(iii) Two eigenvalues of J_{S_3} are $u - \phi N_3 + \frac{\beta R_3}{p + R_3}, \ -\delta_0$ and the other three eigenvalues are the roots of the characteristic equation

$$\varphi^3 + D_1 \varphi^2 + D_2 \varphi + D_3 = 0, \tag{23}$$

where

$$D_1 = \frac{s N_3}{L} + \gamma_0 + \alpha,$$
$$D_2 = \alpha\left(\frac{s N_3}{L} + \gamma_0\right) + \frac{s N_3 \gamma_0}{L} + \theta \lambda N_3\left(1 - \frac{\eta T_3}{l + T_3}\right),$$
$$D_3 = \frac{\alpha s N_3 \gamma_0}{L} + \gamma_0 \theta \lambda N_3\left(1 - \frac{\eta T_3}{l + T_3} - \frac{\eta l T_3}{(l + T_3)^2}\right).$$

All $D_i's (i = 1, 2, 3)$ are positive. Also, we find that $D_1 D_2 - D_3 > 0$. Using the Routh-Hurwitz (R-H) criterion, it is concluded that all roots of equation (23) will fall in left half of the complex plane. Thus, S_3 is unstable whenever $u - \phi N_3 + \frac{\beta R_3}{p + R_3} > 0$.

(iv) The characteristic equation of matrix J_{S^*} is given as

$$\psi^5 + A_1 \psi^4 + A_2 \psi^3 + A_3 \psi^2 + A_4 \psi + A_5 = 0, \tag{24}$$

where

$$A_1 = \alpha + \lambda_1 B^* + \frac{s N^*}{L} + \frac{u B^*}{M} + \gamma_0 + \delta_0,$$

$$A_2 = (\alpha + \lambda_1 B^*)\left(\frac{s N^*}{L} + \frac{u B^*}{M} + \gamma_0 + \delta_0\right) + (\gamma_0 + \delta_0)\left(\frac{s N^*}{L} + \frac{u B^*}{M}\right) + \frac{s N^*}{L}\frac{u B^*}{M}$$
$$+ \gamma_0 \delta_0 + \frac{\beta p B^*}{(p + R^*)^2}(\delta_1 + \delta_2 T^*) + \theta N^* \lambda\left(1 - \frac{\eta T^*}{l + T^*}\right) + \xi N^* \phi B^*,$$

$$A_3 = \gamma_0 \delta_0\left(\alpha + \lambda_1 B^* + \frac{s N^*}{L} + \frac{u B^*}{M}\right) + \left(\frac{s N^*}{L}\frac{u B^*}{M} + \xi N^* \phi B^*\right)(\alpha + \lambda_1 B^* + \gamma_0 + \delta_0)$$
$$+ (\gamma_0 + \delta_0)(\alpha + \lambda_1 B^*)\left(\frac{s N^*}{L} + \frac{u B^*}{M}\right) + \frac{\beta p B^*}{(p + R^*)^2}(\delta_1 + \delta_2 T^*)\left(\alpha + \lambda_1 B^* + \frac{s N^*}{L} + \gamma_0\right)$$
$$+ \theta N^* \lambda\left(1 - \frac{\eta T^*}{l + T^*}\right)\left(\frac{u B^*}{M} + \delta_0\right) + \theta N^* \lambda \gamma_0\left(1 - \frac{\eta T^*}{l + T^*} - \frac{\eta l T^*}{(l + T^*)^2}\right) + \theta N^* \phi B^* \lambda_1 C^*,$$

$$A_4 = \gamma_0 \delta_0 \left[(\alpha + \lambda_1 B^*) \left(\frac{sN^*}{L} + \frac{uB^*}{M} \right) + \frac{sN^*}{L} \frac{uB^*}{M} + \xi N^* \phi B^* \right] + (\gamma_0 + \delta_0) \left[(\alpha + \lambda_1 B^*) \left(\frac{sN^*}{L} \frac{uB^*}{M} \right. \right.$$

$$+ \xi N^* \phi B^*) + \theta N^* \phi B^* \lambda_1 C^* \right] + \frac{\beta p B^*}{(p + R^*)^2} (\delta_1 + \delta_2 T^*) \left[(\alpha + \lambda_1 B^*) \left(\frac{sN^*}{L} + \gamma_0 \right) + \frac{sN^*}{L} \gamma_0 \right]$$

$$+ \theta N^* \lambda \left(1 - \frac{\eta T^*}{l + T^*} \right) \left(\frac{uB^*}{M} \delta_0 + \frac{\beta p B^*}{(p + R^*)^2} (\delta_1 + \delta_2 T^*) \right) + \theta N^* \lambda \gamma_0 \left(\frac{uB^*}{M} + \delta_0 \right) \left(1 - \frac{\eta T^*}{l + T^*} \right)$$

$$- \frac{\eta l T^*}{(l + T^*)^2} \right) - \xi N^* \gamma \lambda \frac{\beta p B^* \delta_2 (M - B^*)}{(p + R^*)^2},$$

$$A_5 = \gamma_0 \delta_0 \left\{ (\alpha + \lambda_1 B^*) \left(\frac{sN^*}{L} \frac{uB^*}{M} + \xi N^* \phi B^* \right) + \theta N^* \lambda_1 C^* \phi B^* \right\} - \frac{\gamma \lambda \beta p B^* \delta_2 (M - B^*)}{(p + R^*)^2}$$

$$\{ (\alpha + \lambda_1 B^*) \xi N^* + \theta N^* \lambda_1 C^* \} + \frac{\gamma_0 \beta p B^*}{(p + R^*)^2} (\delta_1 + \delta_2 T^*) (\alpha + \lambda_1 B^*) \frac{sN^*}{L}$$

$$+ \theta N^* \lambda \gamma_0 \left(\frac{uB^*}{M} \delta_0 + \frac{\beta p B^* (\delta_1 + \delta_2 T^*)}{(p + R^*)^2} \right) \left(1 - \frac{\eta T^*}{l + T^*} - \frac{\eta l T^*}{(l + T^*)^2} \right).$$

Applying the Routh-Hurwitz criterion, the roots of the characteristic equation (24) are either negative or with negative real parts iff the conditions given in (22) are satisfied.

$\square$

Remark 1 The conditions stated in (22) give the necessary and sufficient conditions under which the atmospheric concentration of carbon dioxide, forest biomass and other model variables settle down to a positive equilibrium state as time grows indefinitely if their initial states are close to the equilibrium state.

3.4 Global stability analysis

In the following, the stability analysis of the interior equilibrium S^* is extended to the whole region of attraction Γ using the Lyapunov's direct method [38]. The basic idea of this method for determining the global stability of equilibrium point is to construct a scalar valued positive definite function, called Lyapunov function or energy function, that decreases with time along the trajectories of the system. Using Lyapunov's direct method, we have obtained some sufficient conditions under which the solution trajectories of the system (1) initiating inside the region of attraction converge to S^* as $t \to \infty$. The result regarding the global stability of S^* is stated in the following theorem:

Theorem 2 *The equilibrium S^*, if feasible, is globally asymptotically stable inside the domain Γ if the inequalities given below are satisfied:*

$$\lambda_1^2 C_m{}^2 < \frac{\xi \lambda u}{\theta \phi M} (\alpha + \lambda_1 B^*) \left(1 - \frac{\eta T^*}{l + T^*} \right), \tag{25}$$

$$\frac{\beta R_m^2}{(p + R_m)^2 (p + R^*)} < \frac{u \delta_0}{M (\delta_1 + \delta_2 T^*)}, \tag{26}$$

$$\max \left\{ \frac{\lambda \eta^2 N_m^2}{(l + T^*)^2 (\alpha + \lambda_1 B^*)}, \frac{\xi \beta \delta_2^2 M^2 \left(1 - \frac{\eta T^*}{l + T^*} \right)}{\theta \phi \delta_0 (p + R^*)(\delta_1 + \delta_2 T^*)} \right\} < \frac{8}{9} \frac{s \gamma_0^2}{\theta \lambda^2 \gamma^2 L} \left(1 - \frac{\eta T^*}{l + T^*} \right). \tag{27}$$

Proof Consider the positive definite function $V : \Gamma \to \mathbb{R}$ defined as:

$$V(C, N, B, T, R) = \frac{1}{2} (C - C^*)^2 + m_1 \left(N - N^* - N^* \ln \frac{N}{N^*} \right) + m_2 \left(B - B^* - B^* \ln \frac{B}{B^*} \right)$$

$$+ \frac{m_3}{2} (T - T^*)^2 + \frac{m_4}{2} (R - R^*)^2,$$

where m_1, m_2, m_3 and m_4 are positive constants.

The time derivative of V is given by

$$\dot{V} = -(\alpha + \lambda_1 B^*)(C - C^*)^2 - \frac{m_1 s}{L} (N - N^*)^2 - \frac{m_2 u}{M} (B - B^*)^2 - m_3 \gamma_0 (T - T^*)^2$$

$$- m_4 \delta_0 (R - R^*)^2 - \lambda_1 C (C - C^*)(B - B^*) + \left[\lambda \left(1 - \frac{\eta T^*}{l + T^*} \right) - m_1 \theta \right] (C - C^*)(N - N^*)$$

$$- \frac{\lambda \eta l N}{(l + T)(l + T^*)} (C - C^*)(T - T^*) + (m_1 \xi - m_2 \phi)(N - N^*)(B - B^*)$$

$$+ \left(\frac{m_2 p \beta}{(p + R)(p + R^*)} - m_4(\delta_1 + \delta_2 T^*) \right)(B - B^*)(R - R^*) + m_3 \gamma \lambda (N - N^*)(T - T^*)$$
$$+ m_4 \delta_2 (M - B)(T - T^*)(R - R^*).$$

Choosing $m_1 = \frac{\lambda}{\theta}\left(1 - \frac{\eta T^*}{l + T^*}\right)$ and $m_2 = \frac{m_1 \xi}{\phi} = \frac{\xi \lambda}{\theta \phi}\left(1 - \frac{\eta T^*}{l + T^*}\right)$ and $m_4 = \frac{m_2 \beta}{(p + R^*)(\delta_1 + \delta_2 T^*)} = \frac{\xi \lambda \beta \left(1 - \frac{\eta T^*}{l + T^*}\right)}{\theta \phi (p + R^*)(\delta_1 + \delta_2 T^*)}$, we have

$$\dot{V} = -(\alpha + \lambda_1 B^*)(C - C^*)^2 - \frac{s \lambda}{\theta L}\left(1 - \frac{\eta T^*}{l + T^*}\right)(N - N^*)^2 - \frac{\xi \lambda u}{\theta \phi M}\left(1 - \frac{\eta T^*}{l + T^*}\right)$$

$$(B - B^*)^2 - m_3 \gamma_0 (T - T^*)^2 - \frac{\xi \lambda \beta \delta_0 \left(1 - \frac{\eta T^*}{l + T^*}\right)}{\theta \phi (p + R^*)(\delta_1 + \delta_2 T^*)}(R - R^*)^2 - \lambda_1 C(C - C^*)(B - B^*)$$

$$- \frac{\lambda \eta l N}{(l + T)(l + T^*)}(C - C^*)(T - T^*) - \frac{\xi \lambda \beta R}{\theta \phi (p + R)(p + R^*)}\left(1 - \frac{\eta T^*}{l + T^*}\right)(B - B^*)$$

$$(R - R^*) + m_3 \gamma \lambda (N - N^*)(T - T^*) + \frac{\xi \lambda \beta \delta_2 (M - B)\left(1 - \frac{\eta T^*}{l + T^*}\right)}{\theta \phi (p + R^*)(\delta_1 + \delta_2 T^*)}(T - T^*)(R - R^*).$$

Now, $\dot{V}$ will be negative definite inside Γ under the following inequalities:

$$\lambda_1^2 C_m^2 < \frac{\xi \lambda u}{\theta \phi M}(\alpha + \lambda_1 B^*)\left(1 - \frac{\eta T^*}{l + T^*}\right) \tag{28}$$

$$m_3 > \frac{3}{2} \frac{\lambda^2 \eta^2 N_m^2}{\gamma_0(\alpha + \lambda_1 B^*)(l + T^*)^2} \tag{29}$$

$$\frac{\beta R_m^2}{(p + R^*)(p + R_m)^2} < \frac{u \delta_0}{M(\delta_1 + \delta_2 T^*)} \tag{30}$$

$$m_3 < \frac{4}{3} \frac{s \gamma_0}{\theta \lambda \gamma^2 L}\left(1 - \frac{\eta T^*}{l + T^*}\right) \tag{31}$$

$$m_3 > \frac{3}{2} \frac{\xi \lambda \beta \delta_2^2 M^2}{\theta \phi \gamma_0 \delta_0 (p + R^*)(\delta_1 + \delta_2 T^*)}\left(1 - \frac{\eta T^*}{l + T^*}\right) \tag{32}$$

From inequalities (29), (31) and (32), we can choose $m_3 > 0$ provided condition (27) holds. Thus, the time derivative of V is negative definite inside Γ if conditions (25), (26) and (27) are satisfied. $\square$

Remark 2 The conditions (25)–(27) are the sufficient conditions under which the atmospheric concentration of carbon dioxide and other model variables settle down to positive equilibrium level.

Remark 3 The conditions (25)–(27) may not hold for large values of λ, λ_1, θ and ϕ, indicating that these parameters may have destabilizing effect on dynamic behavior of the system (1).

3.5 Analysis of Hopf-bifurcation

It is noted that on increasing the value of deforestation rate coefficient ϕ, the condition for local stability of interior equilibrium S^* stated in (22) is violated. Thus, there is a possibility of occurrence of Hopf-bifurcation around the equilibrium S^* with respect to the parameter ϕ. Hopf bifurcation is a local bifurcation described by the appearance of a limit cycle around an equilibrium point of system accompanied by a sudden change in stability of the equilibrium point as a parameter of system varies [39]. In the following, we investigate the conditions for the occurrence of Hopf-bifurcation around the equilibrium $S^*(C^*, N^*, B^*, T^*, R^*)$ by considering the deforestation rate coefficient of forest biomass 'ϕ' as bifurcation parameter.

Theorem 3 *The system (1) experiences Hopf-bifurcation around the equilibrium $S^*(C^*, N^*, B^*, T^*, R^*)$ at $\phi = \phi_c$ if the following conditions hold:*

$$(i)\quad \chi(\phi_c) \equiv \{A_3(\phi_c) - A_1(\phi_c)A_2(\phi_c)\}\{A_5(\phi_c)A_2(\phi_c) - A_3(\phi_c)A_4(\phi_c)\}$$
$$- \{A_5(\phi_c) - A_1(\phi_c)A_4(\phi_c)\}^2 = 0,$$

$$(ii)\quad A_1(\phi_c) > 0,\ A_1(\phi_c)A_2(\phi_c) - A_3(\phi_c) > 0,\ A_3(\phi_c) - A_1(\phi_c)\omega_{0c} > 0,$$
$$\omega_{0c} = \frac{A_5(\phi_c) - A_1(\phi_c)A_4(\phi_c)}{A_3(\phi_c) - A_1(\phi_c)A_2(\phi_c)} > 0,$$

$$(iii)\quad \left.\frac{d\chi(\phi)}{d\phi}\right|_{\phi = \phi_c} \neq 0.$$

Proof The characteristic Eq. (24) has purely imaginary roots $\psi_{1,2} = \pm i\sqrt{\omega_0}$, $\omega_0 > 0$ iff it can be rewritten as

$$f(\psi) = (\psi^2 + \omega_0)g(\psi) = 0, where\ g(\psi) = \psi^3 + B_1\psi^2 + B_2\psi + B_3. \tag{33}$$

Thus, we have

$$f(\psi) = \psi^5 + B_1\psi^4 + (B_2 + \omega_0)\psi^3 + (B_3 + B_1\omega_0)\psi^2 + B_2\omega_0\psi + B_3\omega_0 = 0. \tag{34}$$

Equating the coefficients of (24) and (34), we get

$$A_1 = B_1, A_2 = B_2 + \omega_0, A_3 = B_3 + B_1\omega_0, A_4 = B_2\omega_0, A_5 = B_3\omega_0. \tag{35}$$

For the consistence of above relations, we have

$$\omega_0^2 - A_2\omega_0 + A_4 = 0, A_1\omega_0^2 - A_3\omega_0 + A_5 = 0. \tag{36}$$

The elimination of ω_0^2 gives

$$(A_3 - A_1A_2)\omega_0 = A_5 - A_1A_4. \tag{37}$$

Thus (24) can be written as

$$f(\psi) = \psi^5 + A_1\psi^4 + A_2\psi^3 + A_3\psi^2 + \omega_0(A_2 - \omega_0)\psi + \omega_0(A_3 - A_1\omega_0) = 0. \tag{38}$$

If $(A_3 - A_1A_2)$, $(A_5 - A_1A_4) > 0$, then from (37), we have

$$\omega_0 = \omega_{0c} = \frac{A_5 - A_1A_4}{A_3 - A_1A_2} > 0. \tag{39}$$

Substituting $\omega_0 = \omega_{0c}$ in (38), we find that (24) and (38) are identical if and only if

$$\chi = (A_3 - A_1A_2)(A_5A_2 - A_3A_4) - (A_5 - A_1A_4)^2 = 0. \tag{40}$$

Now, the polynomial

$$g(\psi) = \psi^3 + A_1\psi^2 + (A_2 - \omega_0)\psi + A_3 - A_1\omega_0 = 0 \tag{41}$$

does not have zero roots iff

$$A_3 - A_1\omega_0 \neq 0. \tag{42}$$

Now, using Routh-Hurwitz criteria we can infer that all roots of polynomial (41) have negative real parts iff

$$A_1 > 0, A_1A_2 - A_3 > 0, A_3 - A_1\omega_0 > 0. \tag{43}$$

Thus the remaining roots $\psi_{3,4,5}$ of Eq. (34) are either negative or have negative real parts under the condition (43). Now, to show the existence of Hopf-bifurcation, we need to verify the transversality condition.

The function $\chi(\phi)$ can be written in the form of Orlando's formula as:

$$\chi(\phi) = (\psi_1 + \psi_2)(\psi_1 + \psi_3)(\psi_1 + \psi_4)(\psi_1 + \psi_5)(\psi_2 + \psi_3)(\psi_2 + \psi_4)(\psi_2 + \psi_5)$$
$$(\psi_3 + \psi_4)(\psi_3 + \psi_5)(\psi_4 + \psi_5). \tag{44}$$

As $\chi(\phi_c)$ is a continuous function, there exists an open interval $I_{\phi_c} = (\phi_c - \epsilon, \phi_c + \epsilon)$, where ψ_1 and ψ_2 are complex conjugates for all $\phi \in I_{\phi_c}$. Let $\psi_1(\phi) = \zeta_1(\phi) + i\zeta_2(\phi)$, $\psi_2(\phi) = \zeta_1(\phi) - i\zeta_2(\phi)$ with $\zeta_1(\phi_c) = 0$, $\zeta_2(\phi_c) = \sqrt{\omega_0} > 0$ while $\text{Re}(\psi_{3,4,5}(\phi_c)) \neq 0$. Then, we have

$$\chi(\phi) = 2\zeta_1\{(\psi_3 + \zeta_1)^2 + \zeta_2^2\}\{(\psi_4 + \zeta_1)^2 + \zeta_2^2\}\{(\psi_5 + \zeta_1)^2 + \zeta_2^2\}(\psi_3 + \psi_4)(\psi_3 + \psi_5)(\psi_4 + \psi_5),$$
$$\chi(\phi_c) = 0.$$

Differentiating $\chi(\phi)$ with respect to ϕ and then putting $\phi = \phi_c$, we get

$$\left[\frac{d\chi(\phi)}{d\phi}\right]_{\phi=\phi_c} = \left[2(\zeta_2^2 + \psi_3^2)(\zeta_2^2 + \psi_4^2)(\zeta_2^2 + \psi_5^2)(\psi_3 + \psi_4)(\psi_3 + \psi_5)(\psi_4 + \psi_5)\frac{d\zeta_1(\phi)}{d\phi}\right]_{\phi=\phi_c}. \tag{45}$$

Since, at $\phi = \phi_c$, roots $\psi_{3,4,5}$ have negative real part, hence

$$\left[\frac{d\zeta_1(\phi)}{d\phi}\right]_{\phi=\phi_c} \neq 0 \Longleftrightarrow \left[\frac{d\chi(\phi)}{d\phi}\right]_{\phi=\phi_c} \neq 0. \tag{46}$$

Thus the Eq. (46) is the transversality condition. Hence the claim. $\qquad\square$

4 Seasonally forced model

The forest plantation programs are subjected to seasonal variations. Thus, we have taken the implementation rate of reforestation programs δ_1 and the expenditure rate of carbon tax on reforestation programs δ_2 to vary seasonally. By considering time variation in δ_1 and δ_2, system (1) takes the following form:

$$
\begin{aligned}
\dot{C} &= Q + \lambda\left(1 - \frac{\eta T}{l + T}\right)N - \alpha C - \lambda_1 BC, \\
\dot{N} &= sN\left(1 - \frac{N}{L}\right) - \theta CN + \xi NB, \\
\dot{B} &= uB\left(1 - \frac{B}{M}\right) - \phi NB + \frac{\beta RB}{p + R}, \\
\dot{T} &= \gamma(\lambda N) - \gamma_0 T, \\
\dot{R} &= (\delta_1(t) + \delta_2(t)T)(M - B) - \delta_0 R,
\end{aligned}
\tag{47}
$$

Denote $\delta_1^M = \max_{t>0}\delta_1(t)$, $\delta_2^M = \max_{t>0}\delta_2(t)$ and $\delta_1^m = \min_{t>0}\delta_1(t)$, $\delta_2^m = \min_{t>0}\delta_2(t)$.

Lemma 2 *Consider a non-negative, integrable and uniformly continuous function f on $[\kappa, +\infty)$, where κ be a real number, then $\lim_{t\to+\infty} f(t) = 0$.*

4.1 Global attractivity

Theorem 4 *The positive periodic solution of (47), if exists, is unique and globally attractive if $\exists\ \mu_i > 0(i = 1 - 5)$ such that the conditions stated below are satisfied:*

$$
\frac{\mu_1 Q}{e^{2\rho_1}} + \frac{\mu_1 \lambda e^{\rho_{22}}}{e^{2\rho_1}} - \frac{\mu_1 \lambda \eta e^{\rho_2 + \rho_4}}{e^{2\rho_{11}}(l + e^{\rho_{44}})} - \mu_2 \theta > 0,
\tag{48}
$$

$$
\frac{\mu_2 s}{L} - \mu_1\left\{\frac{\lambda}{e^{\rho_{11}}} + \frac{\lambda \eta e^{\rho_4}}{e^{\rho_{11}}(l + e^{\rho_{44}})}\right\} - \mu_3 \phi - \frac{\mu_4 \gamma \lambda}{e^{\rho_{44}}} > 0,
\tag{49}
$$

$$
\frac{\mu_3 u}{M} - \mu_1 \lambda_1 - \mu_2 \xi - \frac{\mu_5 \delta_1^M}{e^{\rho_{55}}} - \frac{\mu_5 \delta_2^M e^{\rho_4}}{e^{\rho_{55}}} > 0,
\tag{50}
$$

$$
\frac{\mu_4 \gamma \lambda e^{\rho_{22}}}{e^{2\rho_4}} - \mu_1 \frac{\lambda \eta l e^{\rho_2}}{e^{\rho_{11}}(l + e^{\rho_{44}})^2} - \frac{\mu_5 \delta_2^M M}{e^{\rho_{55}}} - \frac{\mu_5 \delta_2^M e^{\rho_3}}{e^{\rho_{55}}} > 0,
\tag{51}
$$

$$
\mu_5 \frac{\delta_1^m M}{e^{2\rho_5}} + \mu_5 \frac{\delta_2^m M e^{\rho_{44}}}{e^{2\rho_5}} - \mu_5 \frac{\delta_1^M e^{\rho_3}}{e^{2\rho_{55}}} - \mu_5 \frac{\delta_2^M e^{\rho_3 + \rho_4}}{e^{2\rho_{55}}} - \frac{\mu_3 \beta p}{(p + e^{\rho_{55}})^2} > 0.
\tag{52}
$$

Proof Consider that the system (47) has at least one positive periodic solution $(\overline{C}(t), \overline{N}(t), \overline{B}(t), \overline{T}(t), \overline{R}(t))$. Let

$$
e^{\rho_{11}} \le \overline{C}(t) \le e^{\rho_1}, \ e^{\rho_{22}} \le \overline{N}(t) \le e^{\rho_2}, \ e^{\rho_{33}} \le \overline{B}(t) \le e^{\rho_3}, \ e^{\rho_{44}} \le \overline{T}(t) \le e^{\rho_4}, \ e^{\rho_{55}} \le \overline{R}(t) \le e^{\rho_5}.
$$

Let $(C(t), N(t), B(t), T(t), R(t))$ be any positive periodic solution of the system (47).

We define a Lyapunov functional as,

$$
\begin{aligned}
V(t) =& \mu_1|\ln C(t) - \ln \overline{C}(t)| + \mu_2|\ln N(t) - \ln \overline{N}(t)| + \mu_3|\ln B(t) - \ln \overline{B}(t)| \\
&+ \mu_4|\ln T(t) - \ln \overline{T}(t)| + \mu_5|\ln R(t) - \ln \overline{R}(t)|.
\end{aligned}
$$

Computing the right hand Dini's derivatives, we have

$$
\begin{aligned}
D^+ V(t) =& \mu_1 sgn(C(t) - \overline{C}(t))\left[\frac{\dot{C}(t)}{C(t)} - \frac{\dot{\overline{C}}(t)}{\overline{C}(t)}\right] + \mu_2 sgn(N(t) - \overline{N}(t))\left[\frac{\dot{N}(t)}{N(t)} - \frac{\dot{\overline{N}}(t)}{\overline{N}(t)}\right] \\
&+ \mu_3 sgn(B(t) - \overline{B}(t))\left[\frac{\dot{B}(t)}{B(t)} - \frac{\dot{\overline{B}}(t)}{\overline{B}(t)}\right] + \mu_4 sgn(T(t) - \overline{T}(t))\left[\frac{\dot{T}(t)}{T(t)} - \frac{\dot{\overline{T}}(t)}{\overline{T}(t)}\right] \\
&+ \mu_5 sgn(R(t) - \overline{R}(t))\left[\frac{\dot{R}(t)}{R(t)} - \frac{\dot{\overline{R}}(t)}{\overline{R}(t)}\right].
\end{aligned}
$$

Now, we have

$$\mu_1 sgn(C(t) - \overline{C}(t))\left[\frac{\dot{C}(t)}{C(t)} - \frac{\dot{\overline{C}}(t)}{\overline{C}(t)}\right] \leq \mu_1\left[-\frac{Q}{C(t)\overline{C}(t)}|C(t) - \overline{C}(t)| + \frac{\lambda}{\overline{C}(t)}|N(t) - \overline{N}(t)|\right.$$

$$-\frac{\lambda N(t)}{C(t)\overline{C}(t)}|C(t) - \overline{C}(t)| + \lambda_1|B(t) - \overline{B}(t)|$$

$$+\lambda\eta\left\{\frac{N(t)T(t)}{C(t)\overline{C}(t)(l + T(t))}|C(t) - \overline{C}(t)| + \frac{T(t)}{\overline{C}(t)(l + T(t))}|N(t) - \overline{N}(t)|\right.$$

$$\left.\left.+\frac{l\overline{N}(t)}{\overline{C}(t)(l + T)(l + \overline{T}(t))}|T(t) - \overline{T}(t)|\right\}\right]$$

$$\mu_2 sgn(N(t) - \overline{N}(t))\left[\frac{\dot{N}(t)}{N(t)} - \frac{\dot{\overline{N}}(t)}{\overline{N}(t)}\right] \leq \mu_2\left[-\frac{s}{L}|N(t) - \overline{N}(t)| + \xi|B(t) - \overline{B}(t)|\right.$$

$$+\theta|C(t) - \overline{C}(t)|]$$

$$\mu_3 sgn(B(t) - \overline{B}(t))\left[\frac{\dot{B}(t)}{B(t)} - \frac{\dot{\overline{B}}(t)}{\overline{B}(t)}\right] \leq \mu_3\left[-\frac{u}{M}|B(t) - \overline{B}(t)| + \phi|N(t) - \overline{N}(t)|\right.$$

$$\left.+\frac{\beta p}{(p + R(t))(p + \overline{R}(t))}|R(t) - \overline{R}(t)|\right]$$

$$\mu_4 sgn(T(t) - \overline{T}(t))\left[\frac{\dot{T}(t)}{T(t)} - \frac{\dot{\overline{T}}(t)}{\overline{T}(t)}\right] \leq \mu_4\left[-\frac{\gamma\lambda N(t)}{T(t)\overline{T}(t)}|T(t) - \overline{T}(t)| + \frac{\gamma\lambda}{\overline{T}(t)}|N(t) - \overline{N}(t)|\right]$$

$$\mu_5 sgn(R(t) - \overline{R}(t))\left[\frac{\dot{R}(t)}{R(t)} - \frac{\dot{\overline{R}}(t)}{\overline{R}(t)}\right] \leq \mu_5\left[-\frac{\delta_1(t)(M - B(t))}{R(t)\overline{R}(t)}|R(t) - \overline{R}(t)| + \frac{\delta_1(t)}{\overline{R}(t)}|B(t) - \overline{B}(t)|\right.$$

$$+\frac{\delta_2(t)M}{\overline{R}(t)}|T(t) - \overline{T}(t)| - \frac{\delta_2(t)(M - B(t))T(t)}{R(t)\overline{R}(t)}|R(t) - \overline{R}(t)|$$

$$\left.+\frac{\delta_2(t)T(t)}{\overline{R}(t)}|B(t) - \overline{B}(t)| + \frac{\delta_2(t)\overline{B}(t)}{\overline{R}(t)}|T(t) - \overline{T}(t)|\right].$$

Thus, we have

$$D^+V(t) \leq -\left[\frac{\mu_1 Q}{C(t)\overline{C}(t)} + \frac{\mu_1\lambda N(t)}{C(t)\overline{C}(t)} - \frac{\mu_1\lambda\eta N(t)T(t)}{C(t)\overline{C}(t)(l + T(t))} - \mu_2\theta\right]|C(t) - \overline{C}(t)|$$

$$-\left[\mu_2\frac{s}{L} - \mu_1\left\{\frac{\lambda}{\overline{C}(t)} + \frac{\lambda\eta T(t)}{\overline{C}(t)(l + T(t))}\right\} - \mu_3\phi - \frac{\mu_4\gamma\lambda}{\overline{T}(t)}\right]|N(t) - \overline{N}(t)|$$

$$-\left[\mu_3\frac{u}{M} - \mu_1\lambda_1 - \mu_2\xi - \frac{\mu_5\delta_1(t)}{\overline{R}(t)} - \frac{\mu_5\delta_2(t)T(t)}{\overline{R}(t)}\right]|B(t) - \overline{B}(t)|$$

$$-\left[\frac{\mu_4\gamma\lambda N(t)}{T(t)\overline{T}(t)} - \frac{\mu_1\lambda\eta l\overline{N}(t)}{\overline{C}(t)(l + T(t))(l + \overline{T}(t))} - \frac{\mu_5\delta_2(t)M}{\overline{R}(t)} - \frac{\mu_5\delta_2(t)\overline{B}(t)}{\overline{R}(t)}\right]|T(t) - \overline{T}(t)|$$

$$-\left[\frac{\mu_5\delta_1(t)(M - B(t))}{R(t)\overline{R}(t)} + \frac{\mu_5\delta_2(t)MT(t)}{R(t)\overline{R}(t)} - \frac{\mu_5\delta_2(t)T(t)B(t)}{R(t)\overline{R}(t)} - \frac{\mu_3\beta p}{(p + R(t))(p + \overline{R}(t))}\right]|R(t) - \overline{R}(t)|.$$

Therefore,

$$D^+V(t) \leq -k_1|C(t) - \overline{C}(t)| - k_2|N(t) - \overline{N}(t)| - k_3|B(t) - \overline{B}(t)|$$

$$-k_4|T(t) - \overline{T}(t)| - k_5|R(t) - \overline{R}(t)|, \tag{53}$$

where,

$$k_1 = \frac{\mu_1 Q}{e^{2\rho_1}} + \frac{\mu_1\lambda e^{\rho_{22}}}{e^{2\rho_1}} - \frac{\mu_1\lambda\eta e^{\rho_2 + \rho_4}}{e^{2\rho_{11}}(l + e^{\rho_{44}})} - \mu_2\theta,$$

$$k_2 = \frac{\mu_2 s}{L} - \mu_1 \left\{ \frac{\lambda}{e^{\rho_{11}}} + \frac{\lambda \eta e^{\rho_4}}{e^{\rho_{11}}(l + e^{\rho_{44}})} \right\} - \mu_3 \phi - \frac{\mu_4 \gamma \lambda}{e^{\rho_{44}}},$$

$$k_3 = \frac{\mu_3 u}{M} - \mu_1 \lambda_1 - \mu_2 \xi - \frac{\mu_5 \delta_1^M}{e^{\rho_{55}}} - \frac{\mu_5 \delta_2^M e^{\rho_4}}{e^{\rho_{55}}},$$

$$k_4 = \frac{\mu_4 \gamma \lambda e^{\rho_{22}}}{e^{2\rho_4}} - \mu_1 \frac{\lambda \eta l e^{\rho_2}}{e^{\rho_{11}}(l + e^{\rho_{44}})^2} - \frac{\mu_5 \delta_2^M M}{e^{\rho_{55}}} - \frac{\mu_5 \delta_2^M e^{\rho_3}}{e^{\rho_{55}}},$$

$$k_5 = \mu_5 \frac{\delta_1^m M}{e^{2\rho_5}} + \mu_5 \frac{\delta_2^m M e^{\rho_{44}}}{e^{2\rho_5}} - \mu_5 \frac{\delta_1^M e^{\rho_3}}{e^{2\rho_{55}}} - \mu_5 \frac{\delta_2^M e^{\rho_3 + \rho_4}}{e^{2\rho_{55}}} - \frac{\mu_3 \beta p}{(p + e^{\rho_{55}})^2}.$$

If the conditions (48)–(52) hold, then $V(t)$ is monotonically decreasing on $[0, \infty)$. Now integrating the inequality (53) over $[0, t]$, we get

$$V(t) + \int_0^t [k_1 |C(t) - \overline{C}(t)| + k_2 |N(t) - \overline{N}(t)| + k_3 |B(t) - \overline{B}(t)| + k_4 |T(t) - \overline{T}(t)|$$
$$+ k_5 |R(t) - \overline{R}(t)|] dt \le V(0) < \infty, \forall\, t \ge 0.$$

Using the Lemma 2, we have

$$\lim_{t \to \infty} |C(t) - \overline{C}(t)| = 0, \quad \lim_{t \to \infty} |N(t) - \overline{N}(t)| = 0, \quad \lim_{t \to \infty} |B(t) - \overline{B}(t)| = 0,$$
$$\lim_{t \to \infty} |T(t) - \overline{T}(t)| = 0, \quad \lim_{t \to \infty} |R(t) - \overline{R}(t)| = 0.$$

Hence, the positive periodic solution $(\overline{C}(t), \overline{N}(t), \overline{B}(t), \overline{T}(t), \overline{R}(t))$ is globally attractive.

To prove the uniqueness of globally attractive positive periodic solution $(\overline{C}(t), \overline{N}(t), \overline{B}(t), \overline{T}(t), \overline{R}(t))$, we consider that the system (47) has one more globally attractive solution as $(\overline{C}_1(t), \overline{N}_1(t), \overline{B}_1(t), \overline{T}_1(t), \overline{R}_1(t))$ with period 1. If this solution is different from $(\overline{C}(t), \overline{N}(t), \overline{B}(t), \overline{T}(t), \overline{R}(t))$, then there exists at least one $\kappa \in [0, 1]$ such that $\overline{C}(\kappa) \ne \overline{C}_1(\kappa)$, which means $|\overline{C}(\kappa) - \overline{C}_1(\kappa)| = \epsilon_{11} > 0$. Therefore,

$$\epsilon_{11} = \lim_{n \to \infty} |\overline{C}(\kappa + n) - \overline{C}_1(\kappa + n)|$$
$$= \lim_{t \to \infty} |\overline{C}(t) - \overline{C}_1(t)| > 0,$$

which contradicts the fact that the positive periodic solution $(\overline{C}, \overline{N}, \overline{B}, \overline{T}, \overline{R})$ is globally attractive. Hence, $\overline{C}(t) = \overline{C}_1(t) \, \forall t \in [0, 1]$. We can use the similar arguments for the remaining components $\overline{N}, \overline{B}, \overline{T}$ and $\overline{R}$. Thus, the system (47) has unique globally attractive positive periodic solution. □

5 Numerical simulations

5.1 Simulation of system (1)

To show the impact of integrated carbon taxation-reforestation policy on the atmospheric CO_2 and forest biomass, we have performed numerical simulations using the software environment MATLAB. MATLAB ode solver 'ode45' is used to integrate the system of differential equations (1) [40]. Unless until stated the parameter values in figures will be same as in Table 1. For the given set of parameter values, the eigenvalues of the variational matrix $'J'$ corresponding to the interior equilibrium S^* are given by -3.95993, -0.138065, -0.06631, -0.026177 and -0.012615. Here, we can see that all eigenvalues of J_{S^*} are negative, which means that the interior equilibrium S^* of the system (1) is locally asymptotically stable. The non-linear stability of S^* in $C - B - R$ space is shown in Fig. 3 by taking the parameter values same as in Table 1 except $\lambda = 0.005$, $\phi = 0.00008$, $\lambda_1 = 0.000001$ and $\theta = 0.000001$. From this figure, we may see that the solution trajectories starting at any point inside the region $'\Gamma'$ are approaching to S^*, showing the non-linear stability behavior of the interior equilibrium S^* of system (1) in $C - B - R$ space.

Figure 4 depicts that an increase in the efficacy of carbon taxation policy to cut down the anthropogenic CO_2 emission rate i.e., η causes a decline in equilibrium CO_2 levels. A decrease in half saturation constant l representing the level of carbon taxation at which half of maximum possible reduction in CO_2 emission rate is attained via CO_2 taxation causes decline in the equilibrium CO_2 level. This shows that the taxation policies which leads to higher cuts in CO_2 emission rate at low taxation levels are more beneficial to control atmospheric CO_2 concentration. In Fig. 5, we have drawn contour lines depicting changes in equilibrium CO_2 concentration C^* and forest biomass B^* on varying the imposition rate of carbon tax γ and CO_2 emission rate from human sources λ at a time. It can be seen that the CO_2 settles to low level for high values of imposition rate of carbon tax γ and low values of CO_2 emission rate λ. The equilibrium CO_2 level rises with the rise in anthropogenic CO_2 emission rate, while it declines with the increase in the imposition rate of carbon tax. The second plot of Fig. 5 shows that forest biomass settles to high level for high values of λ and

Fig. 3 Non-linear stability of equilibrium S^* of system (1) in $C - B - R$ space. Other parameters take same values as specified in Table 1 except $\lambda = 0.005$, $\phi = 0.00008$, $\lambda_1 = 0.000001$ and $\theta = 0.000001$
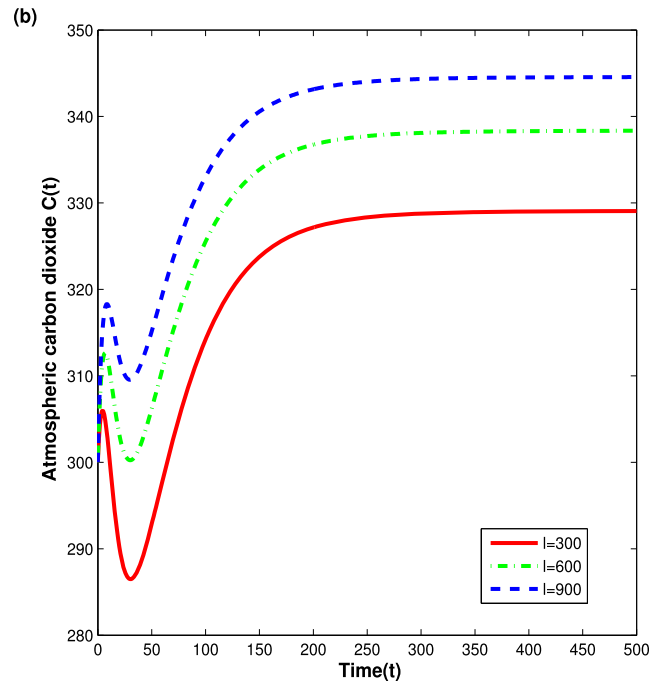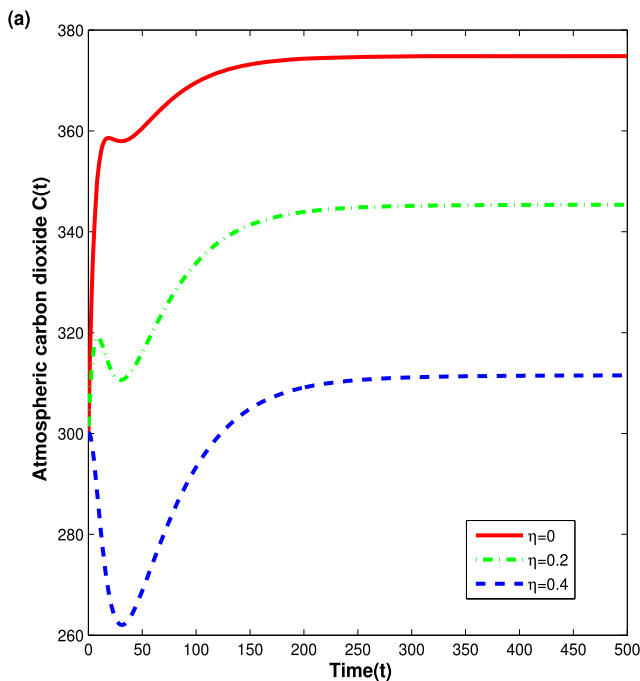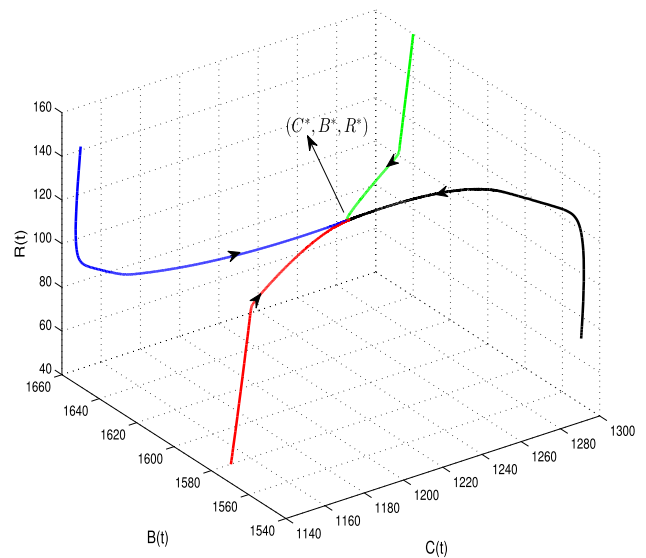

Fig. 4 Variations of atmospheric carbon dioxide with time for different values of η and l for system (1). The other parameters take same values as specified in Table 1

γ. This happens because a part of carbon tax which is imposed on anthropogenic CO_2 emission is invested in reforestation which cause increase in forest biomass.

In Fig. 6, we have plotted the contour lines of equilibrium values C^*, B^*, T^*, and R^* by varying the implementation rate of reforestation programs δ_1 and expenditure rate of carbon tax on reforestation programs δ_2 at a time. This figure depicts a reduction in equilibrium CO_2 concentration and upsurge in equilibrium levels of forest biomass, carbon tax and reforestation programs with an increase in δ_1 and δ_2. It can be observed that for high values of δ_1 and δ_2, the impact of increments in their value over the reduction in C^* and increment in B^* is low in comparison to the scenario when δ_1 and δ_2 are low. This shows that the impact of increase in δ_1 and δ_2 on B^* and C^* saturates at high values of δ_1 and δ_2. Fig. 7 depicts the contour plots of equilibrium levels of CO_2 C^* and forest biomass B^* as a function of maximum efficiency of reforestation programs to enhance forest biomass (β) and deforestation rate coefficient (ϕ). This figure depicts that on increasing the value of β and decreasing the value of ϕ, C^* decreases while B^* increases. Fig. 8 is drawn to show the time evolutions of carbon dioxide and forest biomass in different carbon taxation and reforestation scenarios. From this figure, we can observe that in comparison to the scenario in which only reforestation programs are implemented and the scenario in which carbon taxation is not used to boost the reforestation rate, the increment in equilibrium level of forest
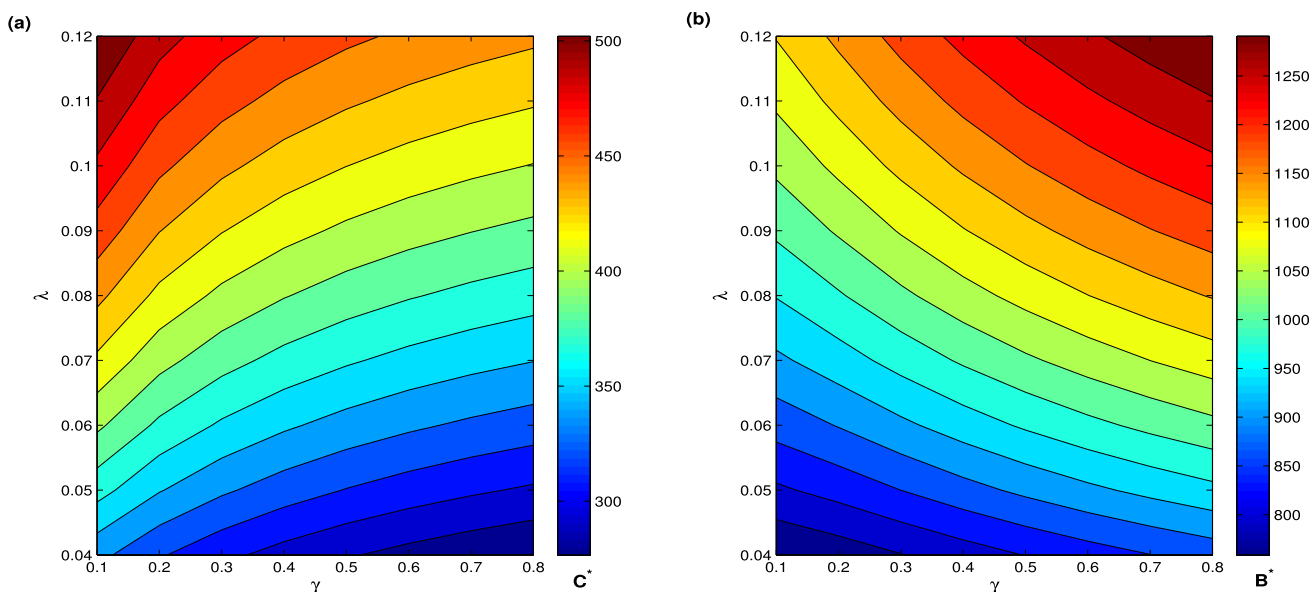
(a)

(b)

Fig. 5 Contour plots of equilibrium level of **a** carbon dioxide (i.e. C^*) and **b** forest biomass (i.e. B^*) as functions of imposition rate of carbon tax γ and per capita anthropogenic emission rate λ for system (1). The other parameters take same values as specified in Table 1

biomass and decline in equilibrium level of CO_2 is more in the scenario when an integrated carbon taxation-reforestation programs is used. This shows that integration of carbon taxation and reforestation policy to boost the implementation rate of reforestation efforts is beneficial to bring down the atmospheric CO_2 levels.

5.1.1 Sensitivity analysis

To study the effect of changes in the parameters η, β, γ, δ_1 and δ_2 on the state variables of system (1), we performed the basic sensitivity analysis of differential equations for the same set of parameter values given in Table 1 following Bortz and Nelson [41]. The sensitivity systems with respect to the parameters η, β, γ, δ_1 and δ_2 are given by

$$\dot{C}_\eta(t, \eta) = \lambda N_\eta(t, \eta) - \frac{\lambda \eta T(t, \eta)}{l + T(t, \eta)} N_\eta(t, \eta) - \frac{\lambda \eta l N(t, \eta)}{(l + T(t, \eta))^2} T_\eta(t, \eta) - \frac{\lambda T(t, \eta) N(t, \eta)}{l + T(t, \eta)}$$
$$- \alpha C_\eta(t, \eta) - \lambda_1 B(t, \eta) C_\eta(t, \eta) - \lambda_1 C(t, \eta) B_\eta(t, \eta),$$

$$\dot{N}_\eta(t, \eta) = s N_\eta(t, \eta) - \frac{2s}{L} N(t, \eta) N_\eta(t, \eta) - \theta C(t, \eta) N_\eta(t, \eta) - \theta N(t, \eta) C_\eta(t, \eta)$$
$$+ \xi N(t, \eta) B_\eta(t, \eta) + \xi B(t, \eta) N_\eta(t, \eta),$$

$$\dot{B}_\eta(t, \eta) = u B_\eta(t, \eta) - \frac{2u}{M} B(t, \eta) B_\eta(t, \eta) - \phi N(t, \eta) B_\eta(t, \eta) - \phi B(t, \eta) N_\eta(t, \eta)$$
$$+ \frac{\beta R(t, \eta)}{p + R(t, \eta)} B_\eta(t, \eta) + \frac{\beta p B(t, \eta)}{(p + R(t, \eta))^2} R_\eta(t, \eta),$$

$$\dot{T}_\eta(t, \eta) = \gamma \lambda N_\eta(t, \eta) - \gamma_0 T_\eta(t, \eta),$$

$$\dot{R}_\eta(t, \eta) = - \delta_1 B_\eta(t, \eta) + \delta_2 M T_\eta(t, \eta) - \delta_2 T(t, \eta) B_\eta(t, \eta) - \delta_2 B(t, \eta) T_\eta(t, \eta)$$
$$- \delta_0 R_\eta(t, \eta),$$

$$\dot{C}_\beta(t, \beta) = \lambda N_\beta(t, \beta) - \frac{\lambda \eta T(t, \beta)}{l + T(t, \beta)} N_\beta(t, \beta) - \frac{\lambda \eta l N(t, \beta)}{(l + T(t, \beta))^2} T_\beta(t, \beta) - \alpha C_\beta(t, \beta)$$
$$- \lambda_1 B(t, \beta) C_\beta(t, \beta) - \lambda_1 C(t, \beta) B_\beta(t, \beta),$$

$$\dot{N}_\beta(t, \beta) = s N_\beta(t, \beta) - \frac{2s}{L} N(t, \beta) N_\beta(t, \beta) - \theta C(t, \beta) N_\beta(t, \beta) - \theta N(t, \beta) C_\beta(t, \beta)$$
$$+ \xi N(t, \beta) B_\beta(t, \beta) + \xi B(t, \beta) N_\beta(t, \beta),$$

$$\dot{B}_\beta(t, \beta) = u B_\beta(t, \beta) - \frac{2u}{M} B(t, \beta) B_\beta(t, \beta) - \phi N(t, \beta) B_\beta(t, \beta) - \phi B(t, \beta) N_\beta(t, \beta)$$
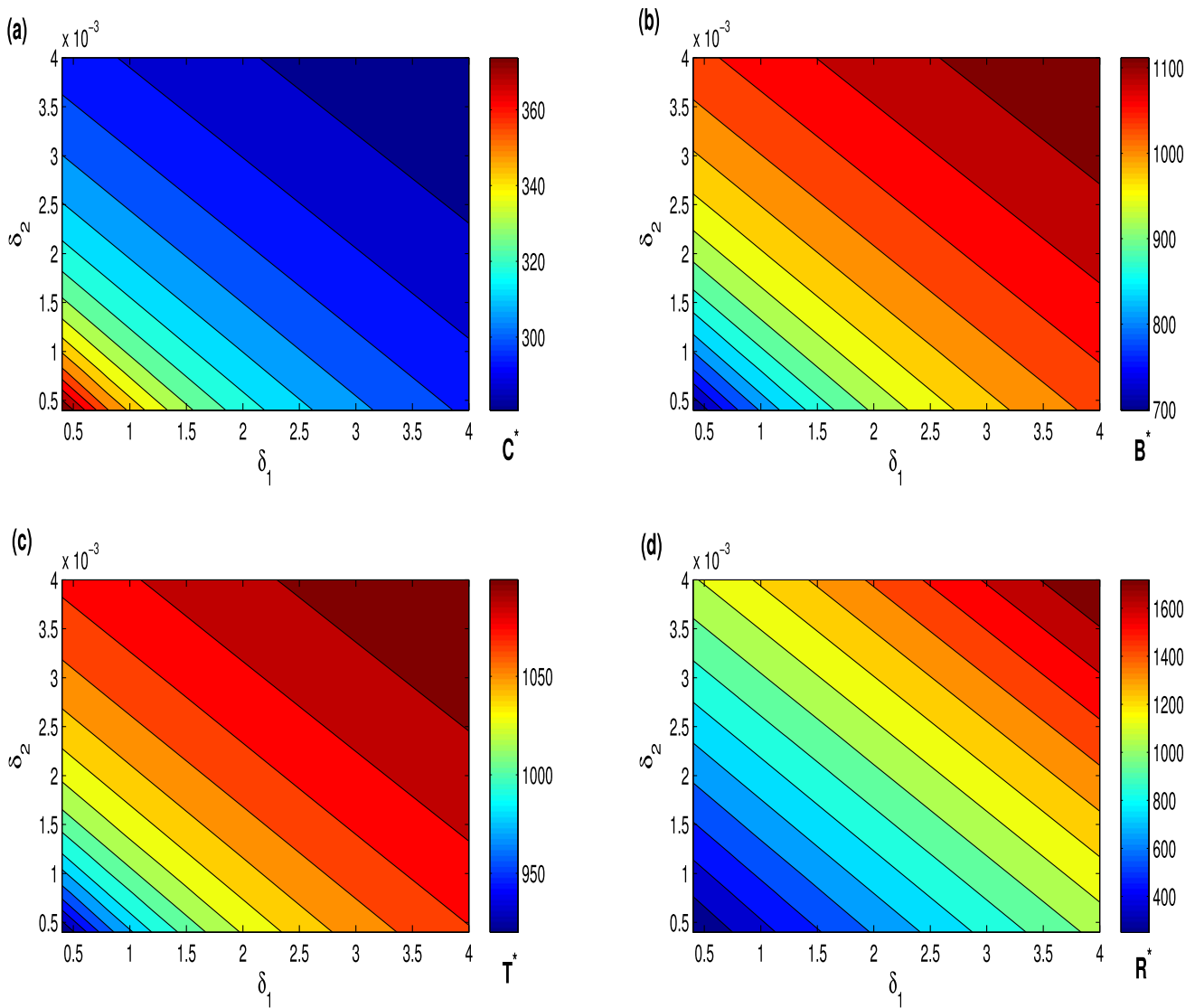
Fig. 6 Contour plots of equilibrium levels of **a** atmospheric carbon dioxide, **b** forest biomass, **c** carbon tax and **d** reforestation programs as functions of δ_1 and δ_2 for system (1). The other parameters take same values as specified in Table 1

$$+ \frac{\beta R(t, \beta)}{p + R(t, \beta)} B_\beta(t, \beta) + \frac{\beta p B(t, \beta)}{(p + R(t, \beta))^2} R_\beta(t, \beta) + \frac{R(t, \beta) B(t, \beta)}{p + R(t, \beta)},$$

$$\dot{T}_\beta(t, \beta) = \gamma \lambda N_\beta(t, \beta) - \gamma_0 T_\beta(t, \beta),$$

$$\dot{R}_\beta(t, \beta) = -\delta_1 B_\beta(t, \beta) + \delta_2 M T_\beta(t, \beta) - \delta_2 T(t, \beta) B_\beta(t, \beta) - \delta_2 B(t, \beta) T_\beta(t, \beta)$$
$$- \delta_0 R_\beta(t, \beta),$$

$$\dot{C}_\gamma(t, \gamma) = \lambda N_\gamma(t, \gamma) - \frac{\lambda \eta T(t, \gamma)}{l + T(t, \gamma)} N_\gamma(t, \gamma) - \frac{\lambda \eta l N(t, \gamma)}{(l + T(t, \gamma))^2} T_\gamma(t, \gamma) - \alpha C_\gamma(t, \gamma)$$
$$- \lambda_1 B(t, \gamma) C_\gamma(t, \gamma) - \lambda_1 C(t, \gamma) B_\gamma(t, \gamma),$$

$$\dot{N}_\gamma(t, \gamma) = s N_\gamma(t, \gamma) - \frac{2s}{L} N(t, \gamma) N_\gamma(t, \gamma) - \theta C(t, \gamma) N_\gamma(t, \gamma) - \theta N(t, \gamma) C_\gamma(t, \gamma)$$
$$+ \xi N(t, \gamma) B_\gamma(t, \gamma) + \xi B(t, \gamma) N_\gamma(t, \gamma),$$

$$\dot{B}_\gamma(t, \gamma) = u B_\gamma(t, \gamma) - \frac{2u}{M} B(t, \gamma) B_\gamma(t, \gamma) - \phi N(t, \gamma) B_\gamma(t, \gamma) - \phi B(t, \gamma) N_\gamma(t, \gamma)$$
$$+ \frac{\beta p B(t, \gamma)}{(p + R(t, \gamma))^2} R_\gamma(t, \gamma) + \frac{\beta R(t, \gamma)}{p + R(t, \gamma)} B_\gamma(t, \gamma),$$
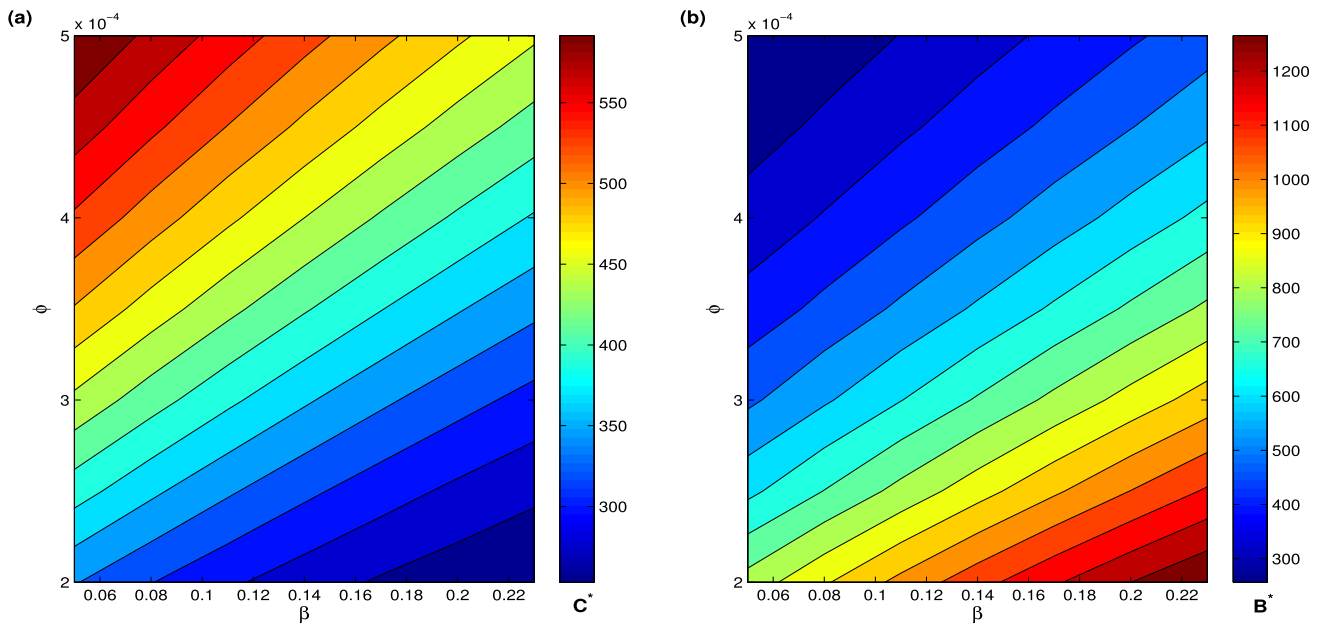
Fig. 7 Contour plots of equilibrium level of **a** carbon dioxide (i.e. C^*) and **b** forest biomass (i.e. B^*) as functions of maximum efficiency of reforestation programs to enhance forest biomass β and deforestation rate coefficient ϕ for system (1). The other parameters take same values as specified in Table 1
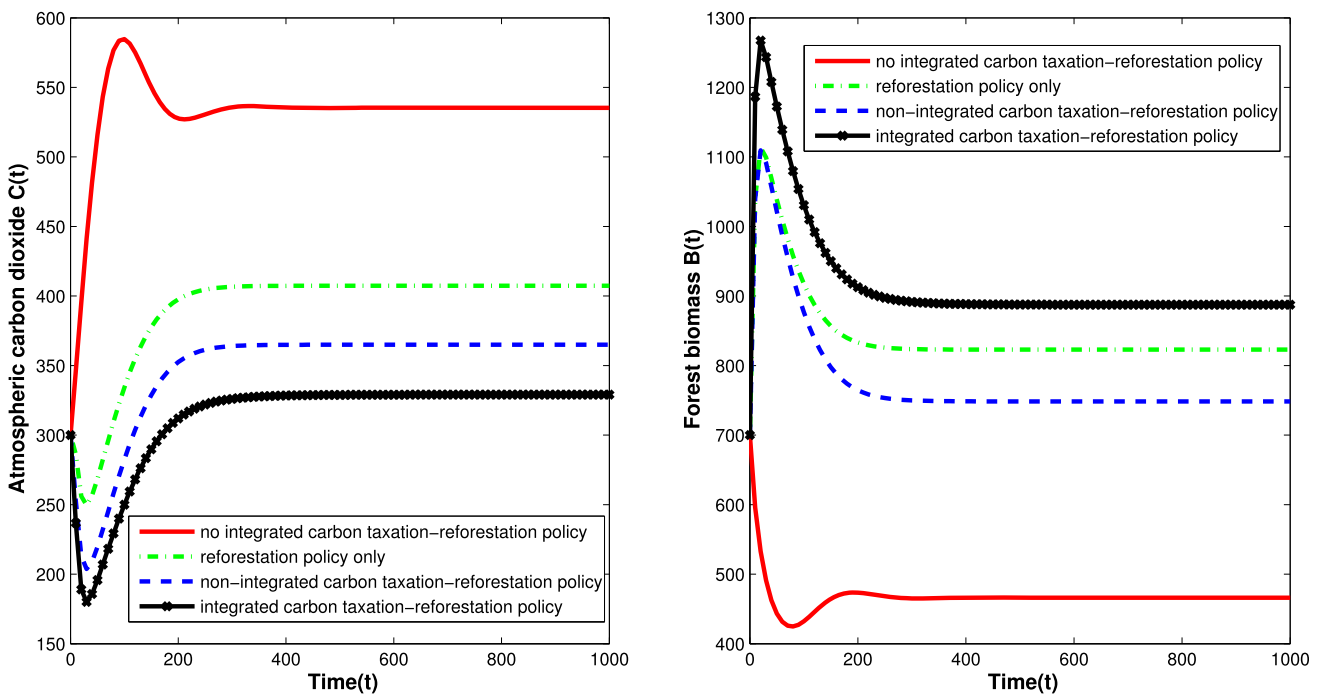

Fig. 8 Time evolutions of carbon dioxide and forest biomass in different carbon taxation and reforestation scenarios. The red solid lines represent the scenario when carbon taxation-reforestation policy is not applied (i.e. system (1) with $\eta = 0$, $l = 0$, $\beta = 0$, $p = 0$, $\gamma = 0$, $\gamma_0 = 0$, $\delta_0 = 0$, $\delta_1 = 0$, and $\delta_2 = 0$), the green dash-dotted lines represent the scenario when only the reforestation policy is applied (i.e. system (1) with $\eta = 0$, $l = 0$, $\gamma = 0$, $\gamma_0 = 0$, and $\delta_2 = 0$), the blue dashed lines represent the scenario when non-integrated taxation-reforestation policy is applied (i.e. system (1) with $\delta_2 = 0$), and the black lines with cross markers represent the scenario when integrated taxation-reforestation policy is applied. The other parameters take same values as specified in Table 1

$$\dot{T}_\gamma(t,\gamma) = \gamma\lambda N_\gamma(t,\gamma) + \lambda N(t,\gamma) - \gamma_0 T_\gamma(t,\gamma),$$

$$\dot{R}_\gamma(t,\gamma) = -\delta_1 B_\gamma(t,\gamma) + \delta_2 M T_\gamma(t,\gamma) - \delta_2 T(t,\gamma)B_\gamma(t,\gamma) - \delta_2 B(t,\gamma)T_\gamma(t,\gamma)$$
$$\qquad -\delta_0 R_\gamma(t,\gamma),$$

$$\dot{C}_{\delta_1}(t,\delta_1) = \lambda N_{\delta_1}(t,\delta_1) - \frac{\lambda\eta T(t,\delta_1)}{l+T(t,\delta_1)}N_{\delta_1}(t,\delta_1) - \frac{\lambda\eta l N(t,\delta_1)}{(l+T(t,\delta_1))^2}T_{\delta_1}(t,\delta_1) - \alpha C_{\delta_1}(t,\delta_1)$$
$$\qquad -\lambda_1 B(t,\delta_1)C_{\delta_1}(t,\delta_1) - \lambda_1 C(t,\delta_1)B_{\delta_1}(t,\delta_1),$$

$$\dot{N}_{\delta_1}(t,\delta_1) = s N_{\delta_1}(t,\delta_1) - \frac{2s}{L}N(t,\delta_1)N_{\delta_1}(t,\delta_1) - \theta C(t,\delta_1)N_{\delta_1}(t,\delta_1) - \theta N(t,\delta_1)C_{\delta_1}(t,\delta_1)$$
$$\qquad + \xi N(t,\delta_1)B_{\delta_1}(t,\delta_1) + \xi B(t,\delta_1)N_{\delta_1}(t,\delta_1),$$

$$\dot{B}_{\delta_1}(t,\delta_1) = u B_{\delta_1}(t,\delta_1) - \frac{2u}{M}B(t,\delta_1)B_{\delta_1}(t,\delta_1) - \phi N(t,\delta_1)B_{\delta_1}(t,\delta_1) - \phi B(t,\delta_1)N_{\delta_1}(t,\delta_1)$$
$$\qquad + \frac{\beta p B(t,\delta_1)}{(p+R(t,\delta_1))^2}R_{\delta_1}(t,\delta_1) + \frac{\beta R(t,\delta_1)}{p+R(t,\delta_1)}B_{\delta_1}(t,\delta_1),$$

$$\dot{T}_{\delta_1}(t,\delta_1) = \gamma\lambda N_{\delta_1}(t,\delta_1) - \gamma_0 T_{\delta_1}(t,\delta_1),$$

$$\dot{R}_{\delta_1}(t,\delta_1) = M - B(t,\delta_1) - \delta_1 B_{\delta_1}(t,\delta_1) + \delta_2 M T_{\delta_1}(t,\delta_1) - \delta_2 T(t,\delta_1)B_{\delta_1}(t,\delta_1) - \delta_2 B(t,\delta_1)T_{\delta_1}(t,\delta_1)$$
$$\qquad -\delta_0 R_{\delta_1}(t,\delta_1),$$

and

$$\dot{C}_{\delta_2}(t,\delta_2) = \lambda N_{\delta_2}(t,\delta_2) - \frac{\lambda\eta T(t,\delta_2)}{l+T(t,\delta_2)}N_{\delta_2}(t,\delta_2) - \frac{\lambda\eta l N(t,\delta_2)}{(l+T(t,\delta_2))^2}T_{\delta_2}(t,\delta_2) - \alpha C_{\delta_2}(t,\delta_2)$$
$$\qquad -\lambda_1 B(t,\delta_2)C_{\delta_2}(t,\delta_2) - \lambda_1 C(t,\delta_2)B_{\delta_2}(t,\delta_2),$$

$$\dot{N}_{\delta_2}(t,\delta_2) = s N_{\delta_2}(t,\delta_2) - \frac{2s}{L}N(t,\delta_2)N_{\delta_2}(t,\delta_2) - \theta C(t,\delta_2)N_{\delta_2}(t,\delta_2) - \theta N(t,\delta_2)C_{\delta_2}(t,\delta_2)$$
$$\qquad + \xi N(t,\delta_2)B_{\delta_2}(t,\delta_2) + \xi B(t,\delta_2)N_{\delta_2}(t,\delta_2),$$

$$\dot{B}_{\delta_2}(t,\delta_2) = u B_{\delta_2}(t,\delta_2) - \frac{2u}{M}B(t,\delta_2)B_{\delta_2}(t,\delta_2) - \phi N(t,\delta_2)B_{\delta_2}(t,\delta_2) - \phi B(t,\delta_2)N_{\delta_2}(t,\delta_2)$$
$$\qquad + \frac{\beta p B(t,\delta_2)}{(p+R(t,\delta_2))^2}R_{\delta_2}(t,\delta_2) + \frac{\beta R(t,\delta_2)}{p+R(t,\delta_2)}B_{\delta_2}(t,\delta_2),$$

$$\dot{T}_{\delta_2}(t,\delta_2) = \gamma\lambda N_{\delta_2}(t,\delta_2) - \gamma_0 T_{\delta_2}(t,\delta_2),$$

$$\dot{R}_{\delta_2}(t,\delta_2) = -\delta_1 B_{\delta_2}(t,\delta_2) + \delta_2 M T_{\delta_2}(t,\delta_2) + M T(t,\delta_2) - \delta_2 T(t,\delta_2)B_{\delta_2}(t,\delta_2) - \delta_2 B(t,\delta_2)T_{\delta_2}(t,\delta_2)$$
$$\qquad - T(t,\delta_2)B(t,\delta_2) - \delta_0 R_{\delta_2}(t,\delta_2),$$

respectively. Here, the semi-relative sensitivity function of X with respect to the parameter w is given by $X_w(t,w) = \frac{\partial}{\partial w}X(t,w)$. The semi-relative sensitivity solutions are calculated by multiplying the sensitivity functions by the parameter w i.e., $wX_w(t,w)$. The semi-relative sensitivity solution gives the information about the change in the state variables when a parameter value is doubled. To show the impact of doubling of parameters η, β, γ, δ_1 and δ_2 on the state variables, semi- relative sensitivity solutions are plotted in Fig 9 for the time period of 100 months. The first plot in Fig. 9 shows that the positive perturbations in the parameters η, β, γ, δ_1 and δ_2 have negative impact on the atmospheric carbon dioxide concentration. A doubling of the parameters η, β and γ lead to decrease of 60.043 ppm, 149.434 ppm and 40.6334 ppm, respectively, in CO_2 concentration, while the doubling of parameters δ_1 and δ_2 lead to decrease of 32.5985 ppm and 31.4580 ppm, respectively, in CO_2 concentration over the period of 100 months. The second plot in Fig. 9 shows that the positive perturbations in the parameters η, β, γ, δ_1 and δ_2 have positive impact on the human population. The third plot in Fig. 9 shows that the positive perturbations in the parameters β, γ, δ_1 and δ_2 have positive impact on the forest biomass, while the positive perturbation in η has negative impact on forest biomass. A doubling of the parameters β, γ, δ_1, δ_2 lead to increase of 570.2917, 95.1760, 124.0634 and 119.6411 million tons, respectively, in the biomass, while the doubling of parameter η lead to decrease of 59.120 million tons, respectively, in the biomass over the period of 100 months. The fourth plot in Fig. 9 shows that the positive perturbations in all the parameters η, β, γ, δ_1 and δ_2 have positive impact on the carbon taxation. The fifth plot in Fig. 9 shows that the positive perturbations in the parameters η, γ, δ_1 and δ_2 have positive impact on the measure of reforestation programs while the positive perturbation in β has negative impact on the measure of reforestation programs. The variables $C(t)$, $N(t)$, $B(t)$ and $R(t)$ are most sensitive to changes in the parameter β while $T(t)$ is most sensitive to the changes in the parameter γ. The sensitivity analysis shows that the parameter β is more influential parameter than η, γ, δ_1 and δ_2 in respect to the control of carbon dioxide concentrations and increment in the forest biomass. This suggests that the selection of reforestation policies greatly influence the carbon dioxide concentrations in the atmosphere.
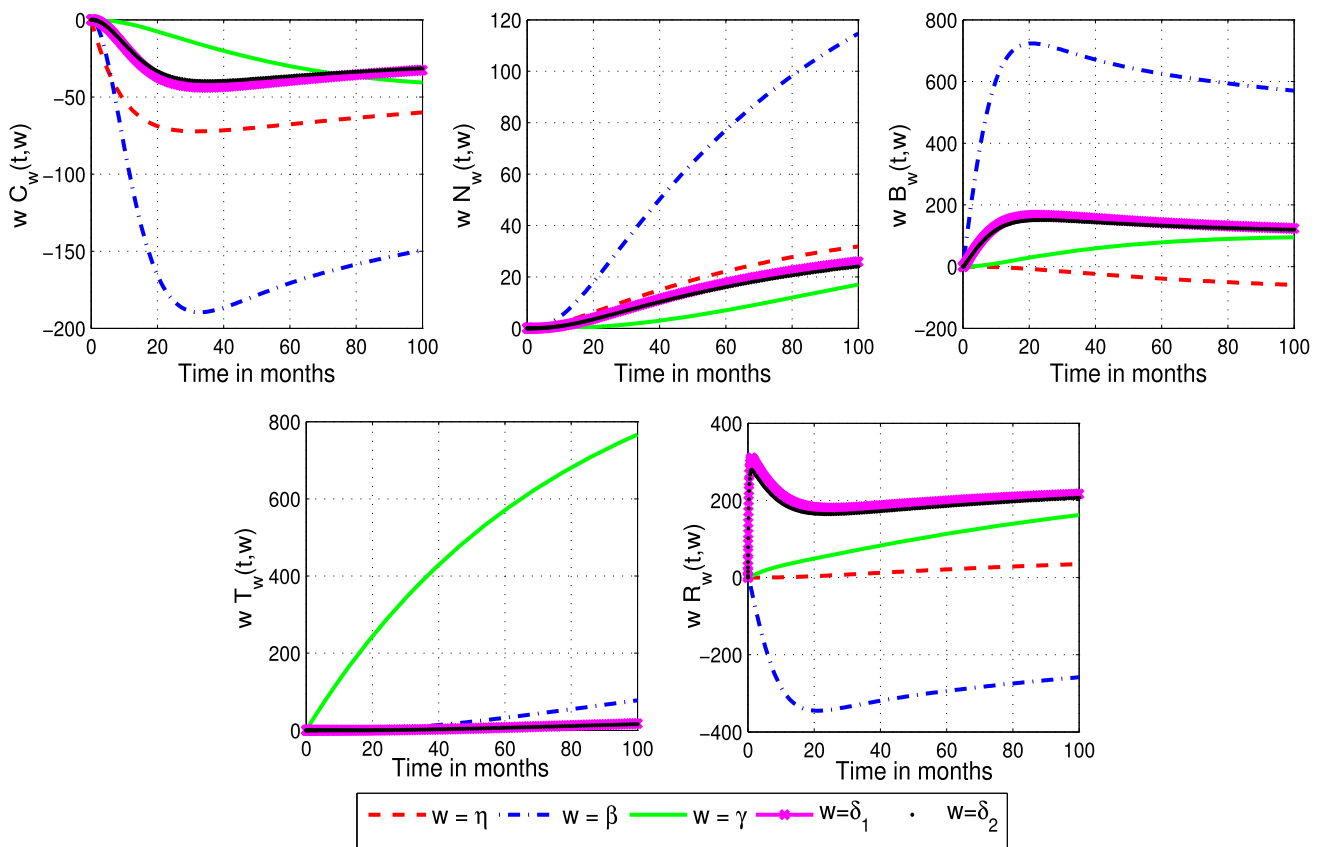
Fig. 9 Semi-relative sensitivity solutions for the state variables of system (1) with respect to parameters η, β, γ, δ_1 and δ_2

5.1.2 Bifurcation results

It is observed that the variations in the deforestation rate ϕ, may significantly influence the dynamical behaviour of system (1). It is found that for $\phi \in (0, \phi_c)$, system (1) exhibits a stable positive equilibrium state S^*. At $\phi = \phi_c$, positive equilibrium state S^* losses stability and periodic oscillations arise via Hopf-bifurcation. The Hopf-bifurcation threshold value is computed to be $\phi_c = 0.0008943$. The variation of $C(t)$, $N(t)$, $B(t)$, $T(t)$ and $R(t)$ with respect to time t for $\phi < \phi_c$ is shown in Fig. 10. This figure illustrates that when $\phi < \phi_c$, all the state variables settle to equilibrium values showing that positive equilibrium state S^* is stable. Further, in Fig. 11, we can see that if $\phi > \phi_c$, system show sustained oscillations around equilibrium S^*. These periodic oscillations may die out and positive equilibrium state S^* again becomes stable if we increase the maximum efficacy of reforestation programs to enhance forest biomass β. Fig. 12 depicts that all the variables of system (1) attain their equilibrium values for $\phi = 0.0009(> \phi_c)$ and $\beta = 0.35$. This means that increment in the maximum efficacy of reforestation programs to enhance forest biomass β exert stabilizing effect of system's dynamics and may cause the interior equilibrium S^* to switch from instablity to stability. In order to present a more clear glimpse of the impact of changes in parameters ϕ and β on the dynamics of system 1, we have drawn the bifurcation diagrams of the system by taking ϕ and β as bifurcation parameters in Figs. 13 and 14 respectively. From Fig. 13, it can be easily seen that when $\phi < \phi_c$, a stable interior equilibrium exists but as ϕ passes through ϕ_c, the interior equilibrium losses stability and periodic oscillations of increasing amplitude developed around interior equilibrium through Hopf-bifurcation. The amplitude of the periodic oscillations declines as the value of β increases. Figure 14 presents the bifurcation diagram of the system by taking β as bifurcation parameter for $\phi = 0.001(> \phi_c)$. From this figure, it is evident that increment in β decreases the amplitude of periodic oscillations that exist for high deforestation rates and after a critical threshold, the periodic oscillations die out and all the variables of system (1) approach their equilibrium values. Thus, we conclude that plantation of plants having high biomass production may not only reduce the atmospheric CO_2 concentration but may also aid in stabilization of atmospheric carbon dioxide concentrations.
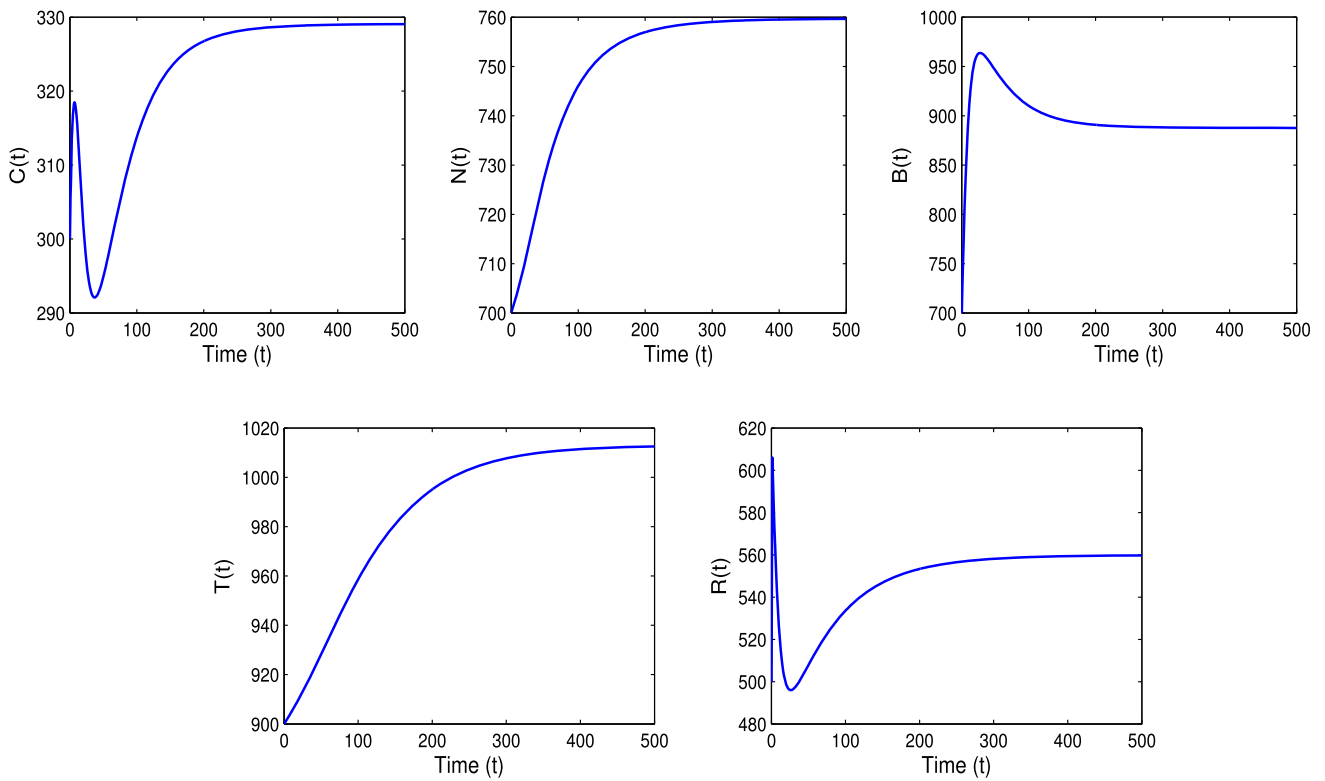
Fig. 10 Time variations of variables of system (1) for ϕ=0.0003. The other parameters take same values as specified in Table 1
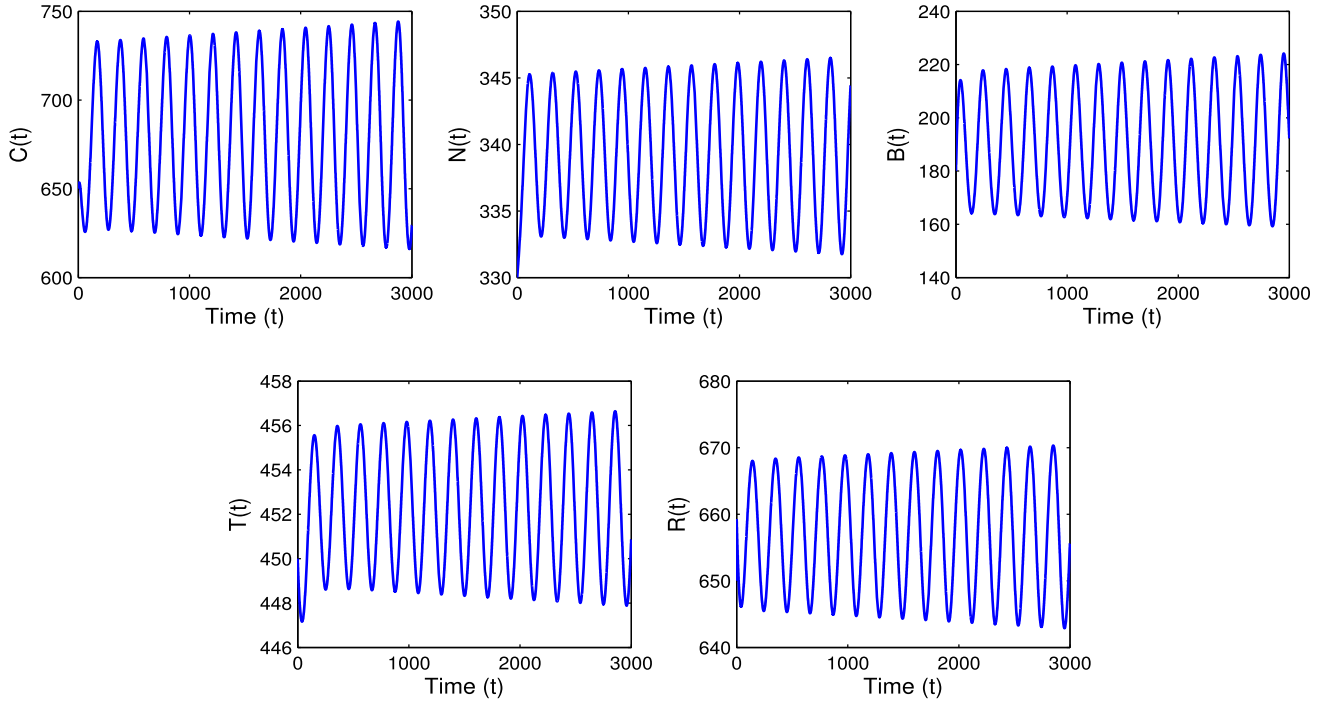

Fig. 11 Time variations of variables of system (1) for ϕ=0.0009. The other parameters take same values as specified in Table 1
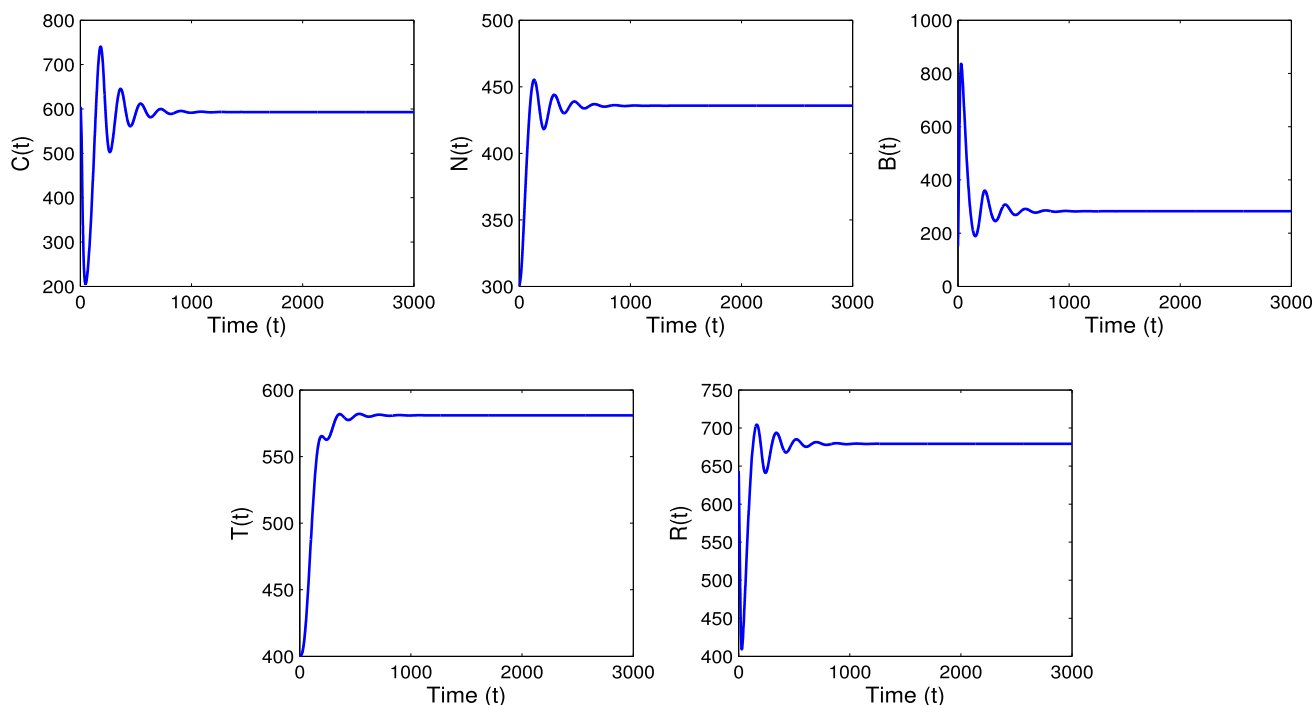
Fig. 12 Time variations of variables of system (1) for ϕ=0.0009 and β=0.35. The other parameters take same values as specified in Table 1
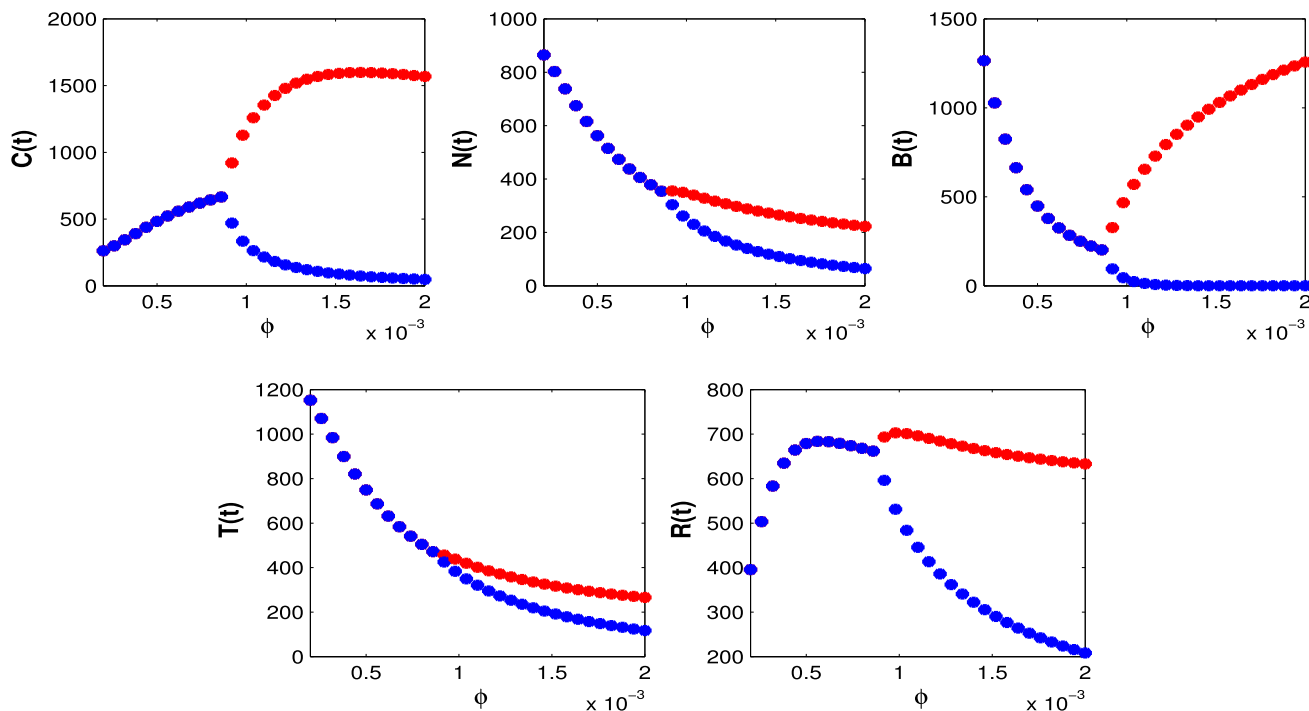

Fig. 13 Bifurcation diagrams of system (1) with respect to ϕ. The other parameters take same values as in Table 1. In this figure, red and blue dots represent the maximum and minimum value of oscillation cycles, respectively

5.2 Simulation of system (47)

To depict the effect of seasonality in plantation efforts on the dynamics of forest biomass and CO_2 levels, we have simulated the nonautonomous system (47) by taking the seasonally forced parameters $\delta_1(t)$ and $\delta_2(t)$ of the form:

$$\delta_1(t) = \delta_1 + \delta_{11} \sin \omega t \text{ and } \delta_2(t) = \delta_2 + \delta_{22} \sin \omega t$$
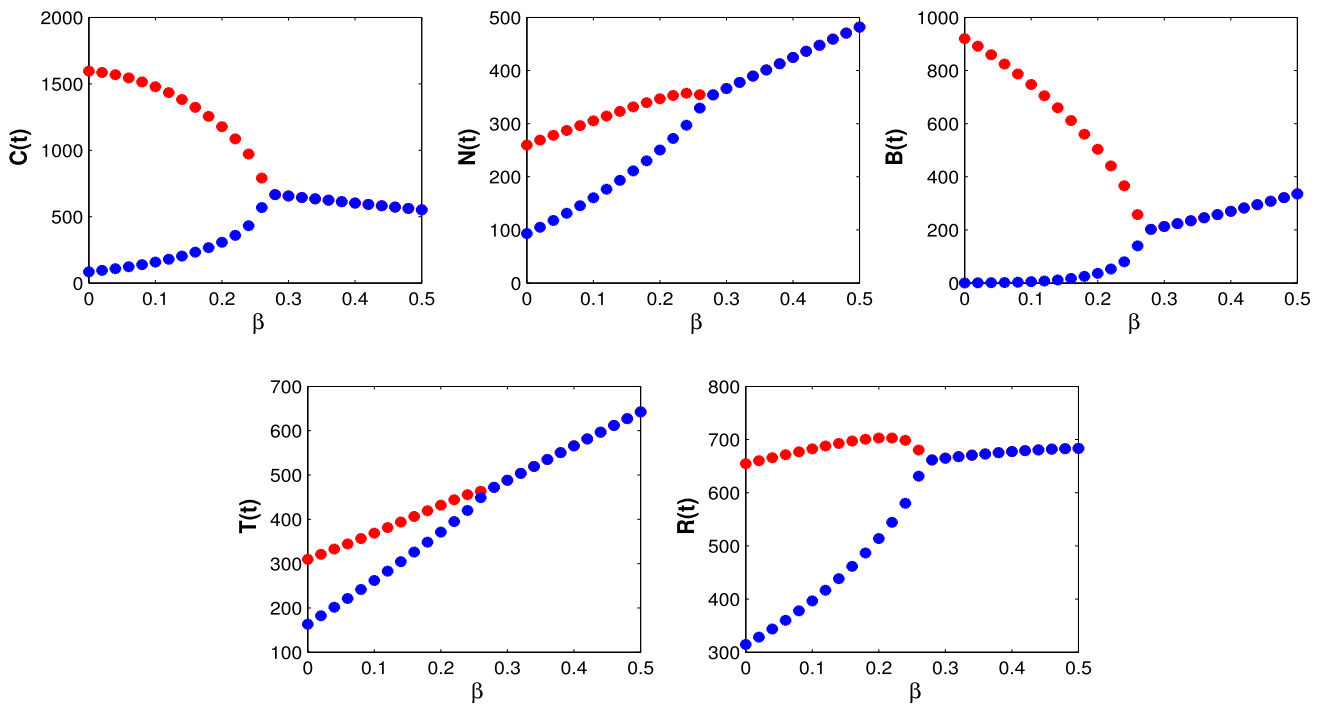
Fig. 14 Bifurcation diagrams of system (1) with respect to β at $\phi = 0.001(> \phi_c)$. The other parameters take same values as in Table 1. In this figure, red and blue dots represent the maximum and minimum value of oscillation cycles, respectively
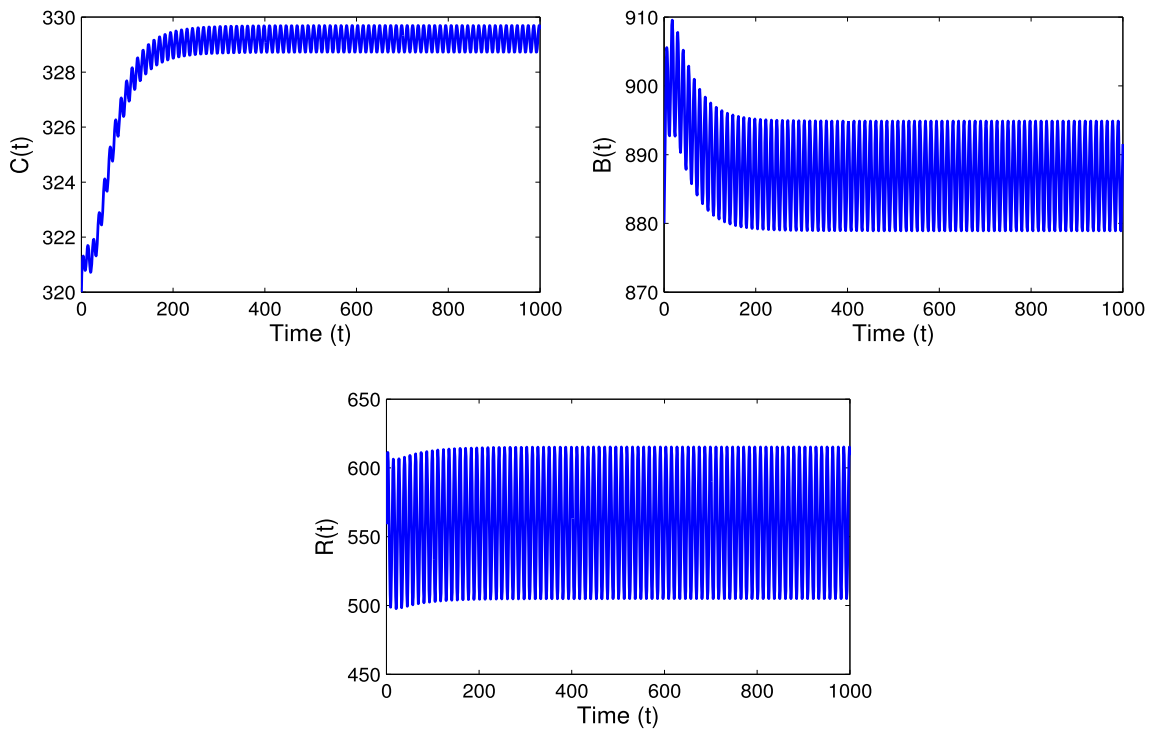

Fig. 15 Time series of $C(t)$, $B(t)$ and $R(t)$ for system (47) at $\delta_{11} = 0.1$, $\delta_{22} = 0.0001$ and $\omega = 2\pi/12$. The other parameters take same values as in Table 1

with a period of 12 months. The benefit of considering the above form of δ_1 and δ_2 is that they encompass both high and low seasons corresponding to positive and negative values of $\sin \omega t$, respectively. Here, parameters $\delta_{11}(0 < \delta_{11} < \delta_1)$ and $\delta_{22}(0 < \delta_{22} < \delta_2)$ decide the strength of seasonal forcing in $\delta_1(t)$ and $\delta_2(t)$, respectively. We have plotted the solution trajectories for the nonautonomous system (47) in Fig. 15 by taking the same set of parameter values specified in Table 1 and $\delta_{11} = 0.1$, $\delta_{22} = 0.0001$, $\omega = 2\pi/12$. This figure shows the periodic oscillations in the non-autonomous system (47), whereas the corresponding autonomous system (1)
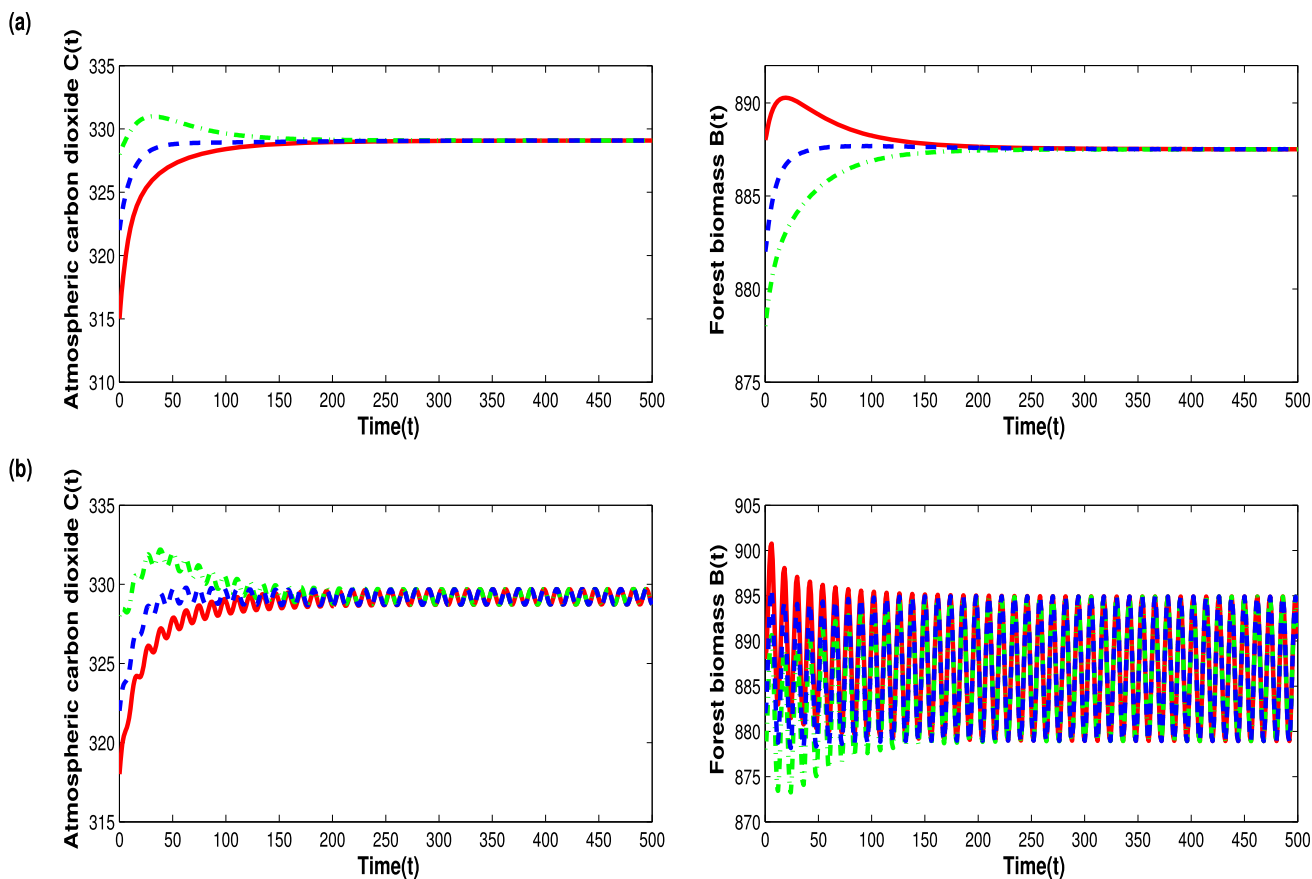
(a)

(b)

Fig. 16 Time series of (**a**) atmospheric carbon dioxide and forest biomass for system (1) and (**b**) atmospheric carbon dioxide and forest biomass for system (47) at $\delta_{11} = 0.1$, $\delta_{22} = 0.0001$ and $\omega = 2\pi/12$ for different initial starts. The other parameters take same values as in Table 1

shows a stable solution (see Fig. 10). Figure 16a and b depict the time evolutions of atmospheric carbon dioxide and forest biomass for three different initial starts for the autonomous system (1) and the non-autonomous system (47) respectively. From the Fig. 16a, it can be noted that for autonomous system, carbon dioxide and forest biomass settle to an equilibrium level irrespective of the initial start, showing the stability of interior equilibrium state of system (1). Figure 16b shows that for the non-autonomous system (47), the solutions initiating from three different initial values converge to a single periodic solution, showing that the system (47) exhibits a globally attractive positive periodic solution. This shows that the inclusion of seasonality in the system cause the translation of the system from having a globally stable interior equilibrium to have a global attractive periodic solutions. Thus, seasonality in plantation programs cause sustained oscillations in the forest biomass and atmospheric carbon dioxide levels. In Fig. 17, we set $\phi = 0.0009$, at which the autonomous system (1) shows a simple periodic solution (see Fig. 11) and consider seasonality in δ_1 and δ_2. It can be seen that for $\phi = 0.0009$, the non-autonomous system shows higher periodic solutions. This shows that the enhancement in the deforestation rate affects the global stability of the nonautonomous system and may lead to generation of higher periodic solutions. The existence of the higher periodic oscillation makes it difficult to predict the future levels of carbon dioxide and forest biomass.

6 Conclusion

Restoring the forest cover can aid in mitigating the climate changes caused by the increase in carbon dioxide levels in the atmosphere. However, several economic and geographical constraints limit the large-scale implementation of reforestation programs. Carbon taxation is another crucial strategy adopted by policymakers that aids to limit anthropogenic carbon dioxide emissions from the point source. A part of the money generated via carbon taxation may be used to boost the implementation rate of plantation programs. Thus, an integrated carbon taxation-reforestation policy may be a better option to control atmospheric CO_2 levels by cutting down anthropogenic CO_2 emissions and overcoming the economic constraints that existed in large-scale plantation programs. This paper presents a mathematical framework to evaluate the effect of integrated carbon taxation-reforestation policy on the mitigation of atmospheric CO_2. The model is formulated by considering five dynamical variables namely, atmospheric concentration of CO_2, human population, forest biomass, carbon tax and reforestation programs. To model the phenomenon, we have assumed that the
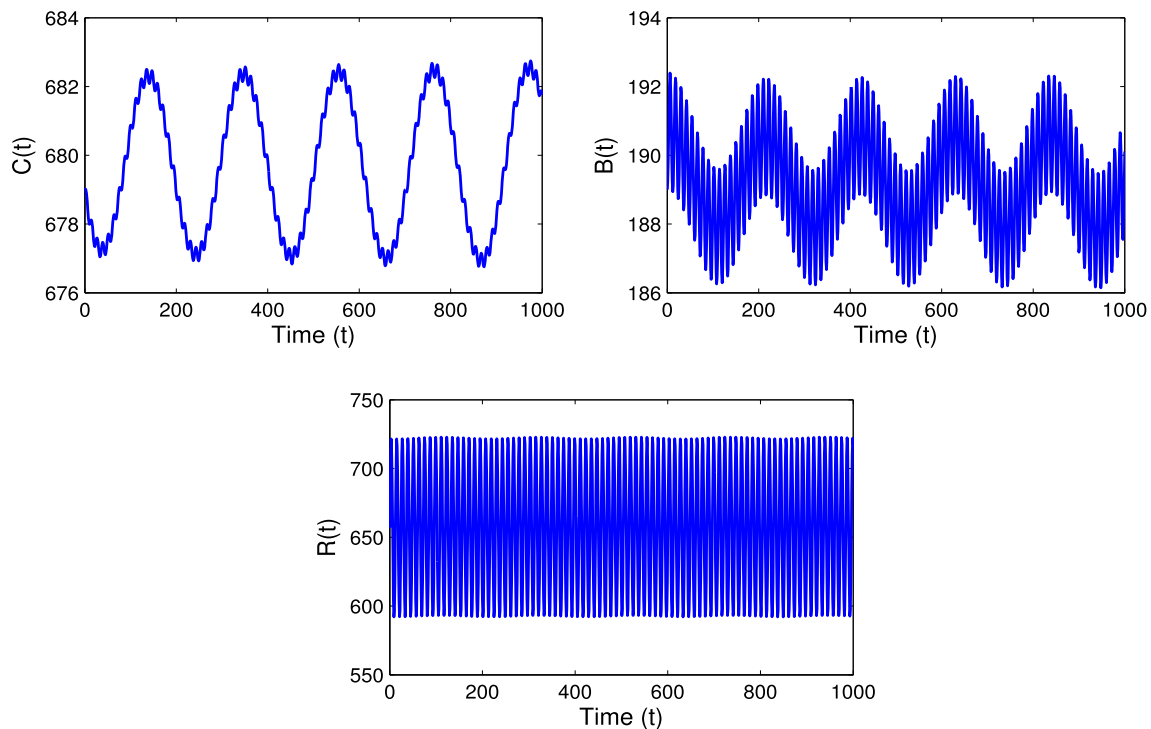
Fig. 17 Time series of $C(t)$, $B(t)$ and $R(t)$ for system (47) at $\delta_{11} = 0.1$, $\delta_{22} = 0.0001$ and $\omega = 2\pi/12$. The other parameters take same values as in Table 1 except $\phi = 0.0009$

carbon tax is implemented on the anthropogenic CO_2 emissions and a part of the money generated via taxation is invested to accelerate the reforestation programs. The qualitative analysis of the model is presented and the local and global stability conditions of the system's equilibria are investigated. Our analysis reveals that increasing the implementation rates of reforestation programs and carbon taxation causes declination in equilibrium CO_2 levels. It is evident that deforestation rate coefficient 'ϕ' may affect the stability of positive equilibrium state S^* of system (1). It is found that an increase in deforestation rate beyond a threshold value ϕ_c destabilizes the positive equilibrium state S^* and system enters into sustained oscillations around S^*. This shows that if deforestation rate exceeds the Hopf-bifurcation threshold ϕ_c, the concentration of carbon dioxide and other model variables will not settle to the equilibrium state but oscillates about the equilibrium level. The amplitude of the periodic oscillations grows as the deforestation rate increase. It is observed that an increment in the maximum efficacy of reforestation programs to enhance forest biomass 'β' can dampen the periodic oscillations and above a threshold value of 'β', periodic oscillations die out and system gets stabilized to a positive equilibrium state. This suggests that reforestation programs that focus on plantation of fast-growing trees high biomass production not only contributes to reduction in atmospheric CO_2 levels but also aids in stabilization of system. It is found that integration of carbon taxation and reforestation programs to boosts the reforestation rate bringing more increment in equilibrium level of forest biomass and decline in equilibrium level of CO_2 in comparison to the scenario in which only reforestation programs are implemented and the scenario in which carbon taxation is not used to boost the reforestation rate.

We have extended our model to examine the effect of seasonal variations in the application of reforestation efforts on the system's dynamics by considering the implementation rate coefficient of reforestation programs and expenditure rate of carbon tax on reforestation programs as a periodic function of time having a period of 12 months. The conditions for the global attractivity of positive periodic solutions of the nonautonomous system are derived. Numerical simulation illustrates that the nonautonomous system possesses globally attractive positive periodic solutions whenever the corresponding autonomous system exhibits stable dynamics. It is found that the high deforestation rates can alter the global attractivity of the periodic solution and the nonautonomous system may show higher periodic solutions at critically high deforestation rates. It is shown that the solution trajectories of the system (47) for different initial starts, when the deforestation rate ϕ is less than the threshold value ϕ_c, converge to a unique periodic solution. This depicts that for a range of deforestation rate, the positive periodic solution is globally asymptotically stable. However, if the deforestation rate is increased above a threshold value, then the system (47) exhibits higher periodic oscillations. Thus, it can be concluded that the high deforestation rate together with the seasonal forcing in application of reforestation efforts is responsible for the generation of higher periodic solution that was absent in the autonomous system. The existence of higher periodic oscillation in the system makes it difficult to predict the future atmospheric level of carbon dioxide and consequently the formulation and implementation of effective reforestation-taxation policy becomes a tedious job. The outcomes of the present investigation suggest that the application of reforestation efforts and carbon tax act as effective control parameters by reducing

the equilibrium level of carbon dioxide. An increase in the efficiency of reforestation programs to increase the forest biomass can alter the prevalence of limit cycle oscillations induced by the high deforestation rate and ultimately lead the system to settle to a stable state. Moreover, the deforestation rate and seasonal variations in the application of reforestation efforts have synergism effect for inducing higher periodic oscillations in the system. For the formulation of an effective integrated carbon taxation-reforestation policy the effects of deforestation rate and seasonal variations in the application of reforestation efforts must be taken into account. Overall, the present study provides a mathematical framework to identify the carbon taxation-reforestation policies for the control of atmospheric CO_2 levels. However, there are several limitations in the current modeling work. One of the main limitations of current modeling framework is that the energy factors and macroeconomic factors that influence carbon tax pricing have not been taken into account. The present work can be extended to include the impact of energy factors and macroeconomic factors on the carbon taxation.

Declarations

Conflict of interest The authors declare that there is no conflict of interest regarding the publication of this article.

Ethical standard The authors state that this research complies with ethical standards. This research does not involve either human participants or animals.

References

1. IPCC, Climate Change 2014: Synthesis Report. Contribution of Working Groups I, II and III to the fifth Assessment Report of the Intergovernmental Panel on Climate Change [Core Writing Team, Pachauri RK, Meyer LA (eds)]. IPCC, Geneva, Switzerland, pp 151 (2014)
2. FAO, Global Forest Resources Assessment 2020: Main report. Rome. https://doi.org/10.4060/ca9825en (2020)
3. K.A. Tafoya, E.S. Brondizio, C.E. Johnson, P. Beck, M. Wallace, R. Quiros, M.D. Wasserman, Effectiveness of Costa Rica's conservation Portfolio to lower deforestation, protect primates, and increase community participation. Front. Environ. Sci. **8**, 580724 (2020)
4. R.B. Jackson, J.S. Baker, Opportunities and constraints for forest climate mitigation. Bioscience **60**, 698–707 (2010)
5. E. Appelbaum, Improving the efficacy of carbon tax policies. J. Gov. Econ. **4**, 100027 (2021)
6. S. Shi, G. Liu, Pricing and coordination decisions in a low-carbon supply chain with risk aversion under a carbon tax. Math. Probl. Eng. **2022**, 769013613 (2022)
7. A. Bruvoll, B.M. Larsen, Greenhouse gas emissions in Norway: Do carbon taxes work? Energy Policy **32**(4), 493–505 (2004)
8. B. Lin, X. Li, The effect of carbon tax on per capita CO_2 emissions. Energy Policy **39**(9), 5137–5146 (2011)
9. F. Brannlund, T. Lundgren, P.O. Marklund, Carbon intensity in production and the effects of climate policy-evidence from Swedish industry. Energy Policy **67**(C), 844–857 (2014)
10. B. Murray, N. Rivers, British Columbia's revenue-neutral carbon tax: a review of the latest grand experiment in environmental policy. Energy Policy **86**, 674–683 (2015)
11. S. Calderon, A.C. Alvarez, A.M. Loboguerrero et al., Achieving CO_2 reductions in Colombia: effects of carbon taxes and abatement targets. Energy Econ. **56**, 575–586 (2016)
12. J.J. Andersson, Carbon taxes and CO_2 emissions: Sweden as a case study. Am. Econ. J. Econ. Pol. **11**(4), 1–30 (2019)
13. G.E. Metcalf, J.H. Stock, The macroeconomic impact of Europe's carbon taxes. NBER Working Paper No. 27488 (2020)
14. A. Ghazounani, W. Xia, M.B. Jabeli, U. Shahzad, Exploring the role of carbon taxation policies on CO_2 emissions: contextual evidence from tax implementation and non-implementation European countries. Sustainability **12**, 8680 (2020)
15. Y. Yu, Z. Jin, J. Li, L. Jia, Research on the impact of carbon tax on CO_2 emissions of China's power industry. Hindawi J. Chem. **2020**, 12 (2020)
16. K. Tennakone, Stability of the biomass-carbon dioxide equilibrium in the atmosphere: mathematical model. Appl. Math. Comput. **35**, 125–130 (1990)
17. K.E. Lonngren, E.W. Bai, On the global warming problem due to carbon dioxide. Energy Policy **36**, 1567–1568 (2008)
18. M.A.L. Caetano, D.F.M. Gherardi, T. Yoneyama, An optimized policy for the reduction of CO_2 emission in the Brazilian Legal Amazon. Ecol. Model. **222**, 2835–2840 (2011)
19. A.K. Misra, M. Verma, A mathematical model to study the dynamics of carbon dioxide gas in the atmosphere. Appl. Math. Comput. **219**, 8595–8609 (2013)
20. A.K. Misra, M. Verma, E. Venturino, Modeling the control of atmospheric carbon dioxide through reforestation: effect of time delay. Model. Earth. Syst. Environ. **1**, 24 (2015)
21. J.B. Shukla, M.S. Chauhan, S. Sundar, R. Naresh, Removal of carbon dioxide from the atmosphere to reduce global warming: a modeling study. Int. J. Glob. Warm. **7**(2), 270–292 (2015)
22. S. Devi, N. Gupta, Dynamics of carbon dioxide gas (CO_2): effects of varying capability of plants to absorb CO_2. Nat. Resour. Model. **32**, e12174 (2018)
23. P. Panja, Deforestation, carbon dioxide increase in the atmosphere and global warming: a modelling study. Int. J. Model. Simul. (2019). https://doi.org/10.1080/02286203.2019.1707501
24. S. Devi, N. Gupta, Comparative study of the effects of different growths of vegetation biomass on CO_2 in crisp and fuzzy environments. Nat. Resour. Model. **33**, e12263 (2020)
25. S. Devi, R.P. Mishra, Preservation of the forestry biomass and control of increasing atmospheric CO_2 using concept of reserved forestry biomass. Int. J. Appl. Comput. Math. **6**, 17 (2020)
26. M. Verma, A.K. Verma, Effect of plantation of genetically modified trees on the control of atmospheric carbon dioxide: a modeling study. Nat. Resour. Model. **34**(2), e12300 (2021)
27. A.K. Misra, A. Jha, Modeling the effect of population pressure on the dynamics of carbon dioxide gas. J. Appl. Math. Comput. **67**(2), 623–640 (2021)

28. M. Verma, A.K. Verma, A.K. Misra, Mathematical modeling and optimal control of carbon dioxide emissions from energy sector. Environ. Dev. Sustain. **23**, 13919–13944 (2021)
29. M. Verma, C. Gautam, Optimal mitigation of atmospheric carbon dioxide through forest management programs: a modeling study. Comput. Appl. Math. **41**, 320 (2022)
30. A.K. Misra, A. Jha, Modeling the effect of budget allocation on the abatement of atmospheric carbon dioxide. Comput. Appl. Math. **41**, 202 (2022)
31. S. Devi, N. Gupta, Effects of inclusion of delay in the imposition of environmental tax on the emission of greenhouse gases. Chaos Solitons Fractals **125**, 41–53 (2019)
32. N.D. Newell, L. Marcus, Carbon dioxide and people. Palaios **2**, 101–103 (1987)
33. K. Onozaki, Population is a critical factor for global carbon dioxide increase. J. Health Sci. **55**, 125–127 (2009)
34. M.S. Nikol'skii, A controlled model of carbon circulation between the atmosphere and the ocean. Comput. Math. Model. **21**, 414–424 (2010)
35. J.M. Hartwick, Deforestation and population increase. In: Institutions, sustainability, and natural resources: institutions for sustainable forest management, chapter 8. Springer, Berlin, pp. 155–191 (2005)
36. H.I. Freedman, J.W.H. So, Global stability and persistence of simple food chains. Math. Biosci. **76**, 69–86 (1985)
37. L. Perko, *Differential Equations and Dynamical Systems*, 3rd edn. (Springer, Berlin, 2000)
38. J.P. LaSalle, S. Lefschetz, *Stability by Lyapunov's Second Method with Applications* (Academic Press, New York, 1961)
39. B.D. Hassard, N.D. Kazarinoff, Y.H. Wan, *Theory and Applications of Hopf-Bifurcation* (Cambridge University Press, Cambridge, 1981)
40. ode45: Solve nonstiff differential equations-medium order method, https://in.mathworks.com/help/matlab/ref/ode45.html
41. D.M. Bortz, P.W. Nelson, Sensitivity analysis of a nonlinear lumped parameter model of HIV infection dynamics. Bull. Math. Biol. **66**, 1009–1026 (2004)